Available online at www.sciencedirect.com
ScienceDirect
ELSEVIER
Palaeogeography, Palaeoclimatology, Palaeoecology 241 (2006) 457–491
PALAEO
www.elsevier.com/locate/palaeo

Palaeoenvironment and palaeoclimate of the Middle Miocene lake in the Steinheim basin, SW Germany: A reconstruction from C, O, and Sr isotopes of fossil remains

T. Tütken [a,b,*], T.W. Vennemann [b], H. Janz [c], E.P.J. Heizmann [d]

[a] *Institut für Geowissenschaften, Geochemie, Universität Tübingen, Wilhelmstrasse 56, 72074 Tübingen, Germany*
[b] *Institut de Minéralogie et Géochimie, Université de Lausanne, UNIL–BFSH 2, 1015 Lausanne, Switzerland*
[c] *Rappenberghalde 82, 72070 Tübingen, Germany*
[d] *Staatliches Museum für Naturkunde Stuttgart am Löwentor, Rosenstein 1, 70191 Stuttgart, Germany*

Received 23 November 2005; received in revised form 30 March 2006; accepted 27 April 2006

Abstract

A differentiated reconstruction of palaeolimnologic, –environmental, and –climatic conditions is presented for the Middle Miocene long-term freshwater lake (14.3 to 13.5 Ma) of the Steinheim basin, on the basis of a combined C, O, and Sr isotope study of sympatric skeletal fossils of aquatic and terrestrial organisms from the lake sediments.

The oxygen isotope composition for lake water of the Steinheim basin ($\delta^{18}O_{H2O}$=+2.0±0.4‰ VSMOW, n=6) was reconstructed from measurements of $\delta^{18}O_{PO4}$ of aquatic turtle bones. The drinking water calculated from the enamel of large mammals (proboscideans, rhinocerotids, equids, cervids, suids) has $\delta^{18}O_{H2O}$ values ($\delta^{18}O_{H2O}$=−5.9±1.7‰ VSMOW, n=31) typical for Middle Miocene meteoric water of the area. This $\delta^{18}O_{H2O}$ value corresponds to a mean annual air temperature (MAT) of 18.8±3.8 °C, calculated using a modern-day $\delta^{18}O_{H2O}$-MAT relation. Hence, large mammals did not use the lake water as principal drinking water. In contrast, small mammals, especially the then abundant pika *Prolagus oeningensis* drank from ^{18}O-enriched water sources ($\delta^{18}O_{H2O}$=+2.7±2.3‰ VSMOW, n=7), such as the lake water. Differences in Sr and O isotopic compositions between large and small mammal teeth indicate different home ranges and drinking behaviour and support migration of some large mammals between the Swabian Alb plateau and the nearby Molasse basin, while small mammals ingested their food and water locally.

Changes in the lake level, water chemistry, and temperature were inferred using isotopic compositions of ostracod and gastropod shells from a composite lake sediment profile. Calcitic ostracod valves (*Ilyocypris binocularis*; $\delta^{18}O$=+1.7±1.2‰ VPDB, $\delta^{13}C$=−0.5±0.9‰, VPDB, n=68) and aragonitic gastropod shells (*Gyraulus* spp.; $\delta^{18}O$=+2.0±1.3‰ VPDB, $\delta^{13}C$=−1.1±1.3‰ VPDB, n=89) have $\delta^{18}O$ and $\delta^{13}C$ values similar to or even higher than those of marine carbonates. $\delta^{13}C$ values of the biogenic carbonates parallel lake level fluctuations while $\delta^{18}O$ values scatter around +2±2‰ and reflect the short term variability of meteoric water inflow vs. longer term evaporation. $^{87}Sr/^{86}Sr$ ratios of aragonitic *Gyraulus* spp. gastropod shells parallel the lake level fluctuations, reflecting variable inputs of groundwater and surface waters. Using a water $\delta^{18}O_{H2O}$ value of +2.0‰ VSMOW, water temperatures calculated from skeletal tissue $\delta^{18}O$ values of ostracods are 16.7±5.0 °C, gastropods 20.6±5.6 °C, otoliths 21.8±1.4 °C, and fish teeth 17.0±2.7 °C.

* Corresponding author. Institut für Geowissenschaften, Geochemie, Universität Tübingen, Wilhelmstrasse 56, 72074 Tübingen, Germany. Tel.: +49 7071 29 73 156.
E-mail address: thomas.tuetken@uni-tuebingen.de (T. Tütken).

0031-0182/$ - see front matter © 2006 Elsevier B.V. All rights reserved.
doi:10.1016/j.palaeo.2006.04.007

The calculated MAT (~19 °C), lake water temperatures (~17 to 22 °C) and the ^{18}O-enriched water compositions are indicative of warm-temperate climatic conditions, possibly with a high humidity during this period. Vegetation in the area surrounding the basin was largely of the C_3-type, as indicated by carbon isotopic compositions of tooth enamel from large mammals ($\delta^{13}C = -11.1 \pm 1.1$‰ VPDB, $n = 40$).
© 2006 Elsevier B.V. All rights reserved.

Keywords: Mammal teeth; Oxygen isotopes; Strontium isotopes; Palaeoclimate; Gastropods; Ostracods

1. Introduction

Detailed reconstruction of past changes in environmental or climatic conditions are largely based on high-resolution studies of proxies in marine sediment cores (e.g., Miller et al., 1991; Lear et al., 2000; Zachos et al., 2001). For the terrestrial realm such reconstructions are more difficult to obtain and high-resolution archives such as ice cores, speleothems or lake sediments are mostly restricted to the Quaternary. For pre-Quaternary periods such reconstructions of terrestrial palaeoenvironments and palaeoclimates are commonly based on palaeosols (e.g., Retallack, 2004), fossil plants (e.g., Eberhard, 1989; Lücke et al., 1999; Utescher et al., 2000), vertebrate occurrences (e.g., Markwick, 1998; Jernvall and Fortelius, 2002; Böhme, 2003, 2004), or the isotopic compositions of soil or biogenic carbonates (e.g., Quade et al., 1992; Patterson et al., 1993; Swart et al., 1993; Patterson, 1999 and references therein; Dettmann et al., 2001; Janz and Vennemann, 2005), and mammal bones and teeth (Luz et al., 1984; Longinelli, 1984; Luz and Kolodny, 1985; Longinelli, 1995; Fricke and O'Neil, 1996; Fricke et al., 1998; MacFadden et al., 1999; Kohn and Cerling, 2002; Lindars et al., 2003). The carbon and oxygen isotopic composition of biogenic apatite such as mammalian tooth enamel has proven itself as a valuable archive for reconstructions of past climatic and environmental changes (Cerling et al., 1997; Sharp and Cerling, 1998; Fricke et al., 1998; Koch, 1998; Kohn and Cerling, 2002; Grimes et al., 2005). Such archives from mammals can be combined with measurements from biogenic carbonates formed by sympatric freshwater organisms in order to allow for both the reconstruction of past mean annual air temperatures and summer season temperatures, as well as the oxygen isotope composition of freshwater for Tertiary settings (e.g., Grimes et al., 2003, 2005).

A detailed palaeoenvironmental and palaeoclimatic reconstruction for the Middle Miocene long-term freshwater lake of the Steinheim basin is presented on the basis of a multi-proxy C, O, and Sr isotopic approach of analysing biogenic carbonate as well as phosphatic fossils from autochthonous aquatic as well as sympatric terrestrial species, including mammals, fish, aquatic turtles, ostracods, and gastropods. The Steinheim basin has been palaeontologically and sedimentologically well characterized (e.g., review in Heizmann and Reiff, 2002), as it represents the international reference locality for the European Neogene Mammal assemblage zone MN 7 (~13.5 Ma) in the Middle Miocene, a period with significant global changes in climatic conditions (e.g., Flower and Kennett, 1994; Zachos et al., 2001; Böhme, 2003).

In this study the meteoric and lake water $\delta^{18}O_{H2O}$ values will be reconstructed from mammalian tooth enamel and aquatic turtle bone phosphate $\delta^{18}O_{PO4}$ values and used as proxies for vertebrate drinking water compositions (e.g., Longinelli, 1984, 1995; Barrick et al., 1999; Grimes et al., 2003). On the basis of the reconstructed lake water $\delta^{18}O_{H2O}$ value, water temperatures are calculated using well-preserved carbonaceous and phosphatic skeletal remains of freshwater organisms. Implications from enamel carbon, oxygen, and strontium isotope data for the drinking and feeding behaviour of large vs. small mammals will also be discussed.

2. Geologic setting of the Steinheim basin

2.1. Formation and age of the basin

The Steinheim basin is a small Tertiary sedimentary basin, situated on the Upper Jurassic limestone plateau of the Swabian Alb in SW Germany (Fig. 1). The basin was formed by a meteorite impact during the Middle Miocene (Dietz, 1959; Engelhardt et al., 1967). The impact was presumably simultaneous with that forming the larger Nördlinger Ries crater (Shoemaker and Chao, 1961; Reiff, 1988; Schudack and Janz, 1997) situated 40 km further east on the Swabian Alb plateau (Fig. 1). The Ries crater was dated with various methods to around 15 Ma (K/Ar: 14.8±0.6 Ma, Gentner et al., 1963, and fission track: 14.7±0.7 Ma, Gentner and Wagner, 1969; $^{40}Ar/^{39}Ar$: 15.1±0.1 Ma, Staudacher et al., 1982). However, more recent $^{40}Ar/^{39}Ar$ dates

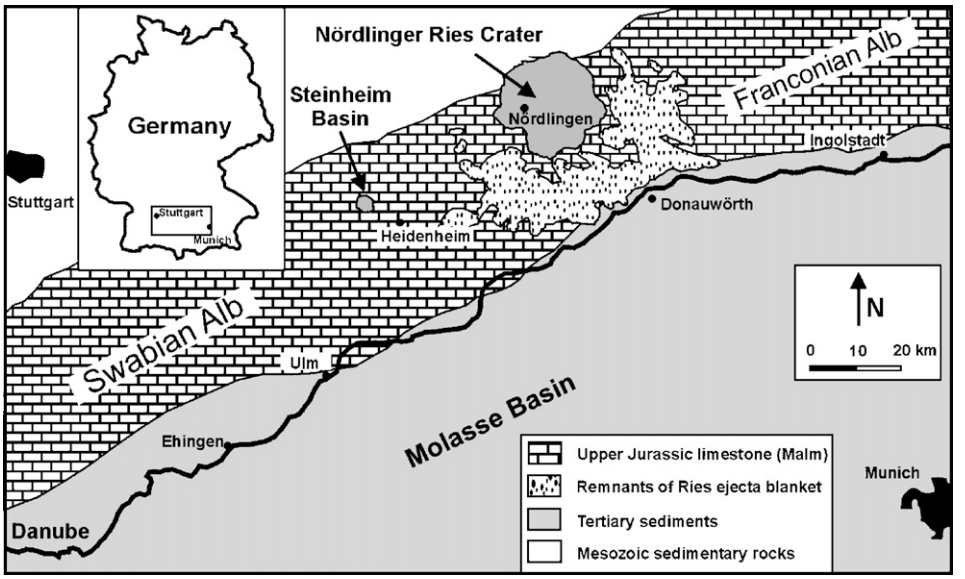

Fig. 1. Simplified geological map of the Swabian and Franconian Alp region with the contemporaneously formed Middle Miocene meteorite impact crater basins of Steinheim and the Nördlinger Ries in the Upper Jurassic limestone plateau, modified after Buchner et al. (2003).

suggested an age for the Ries impact (and thus the formation of the Steinheim basin) of 14.3±0.2 Ma (Buchner et al., 2003, Fig. 2a).

2.2. Evolution of the freshwater lake and stratigraphy of lake sediments

The Steinheim basin is a complex impact crater of 3.5 km diameter and an original depth of about 220 m. It has an almost circular outline and a central elevation (Reiff, 1976). The bottom of the basin is covered by a 40–50 m thick polymict impact breccia consisting of Jurassic limestone blocks with a clayey matrix, which sealed the cleaved and karstic Upper Jurassic limestone (Mensink, 1984). The Steinheim basin was successively filled by meteoric water, forming an oligotrophic lake. The lake in the Steinheim Basin existed for at least a few 100 ka up to more than 1 Ma (Gorthner and Meier-Brook, 1985; Reiff, 1988; Gorthner, 1992). The Nördlinger Ries was also filled by a long-term lake that probably existed for 0.3 up to 2 Ma (Jankowski, 1981 and references therein). But in contrast to the Steinheim basin, the Ries Lake is considered to have been an evaporative saline shallow-water lake (Rothe and Hoefs, 1977; Jankowski, 1981).

As there is no evidence for any river in- or outflow, the Steinheim basin is generally assumed to have been an isolated basin with a water supply mainly from subterranean karst systems and/or surface runoff (Reiff, 1988). The lake level fluctuated significantly (Mensink, 1984; Bahrig et al., 1986), related both to tectonic movements of the Swabian Alb (Reiff, 1988) as well as a function of evaporation (Bajor, 1965). The lake level fluctuations had an important influence on the ecosystem of Lake Steinheim and its faunal evolution, especially the freshwater gastropod and ostracod fauna (Mensink, 1984; Gorthner, 1992; Janz, 1992, 1997, 2000) as well as on the chemical and isotopic composition of the lake water (Bajor, 1965; Wolff and Füchtbauer, 1976).

Detrital input into the Steinheim basin was negligible and the sedimentation rate was low, as reflected by the dominant deposition of lacustrine carbonates such as aragonitic siltstones, arenites and limestones of different degrees of consolidation (Wolff and Füchtbauer, 1976; Mensink, 1984; Bahrig et al., 1986). The basin facies is characterized by gyttjas while the littoral rim facies is made up of biogenic carbonate sands and silts and green algae bioherms around the central hill (Groschopf and Reiff, 1969; Bahrig et al., 1986). Calcareous sediments contain predominantly bioclasts, mainly aragonitic gastropod shells and characean pieces but also ostracods and carbonate grains as sub-mm sized fecal pellets and aragonite-cemented particles (Wolff and Füchtbauer, 1976). The unusual preservation of aragonite may be related to Mg^{2+}-rich and aragonite-saturated pore fluids from dolomite weathering of the dolomitized bioherms (Wolff and Füchtbauer, 1976). The lake deposits can not be lithostratigraphically subdivided and contain only a few marker horizons such as one leaf layer and two fish

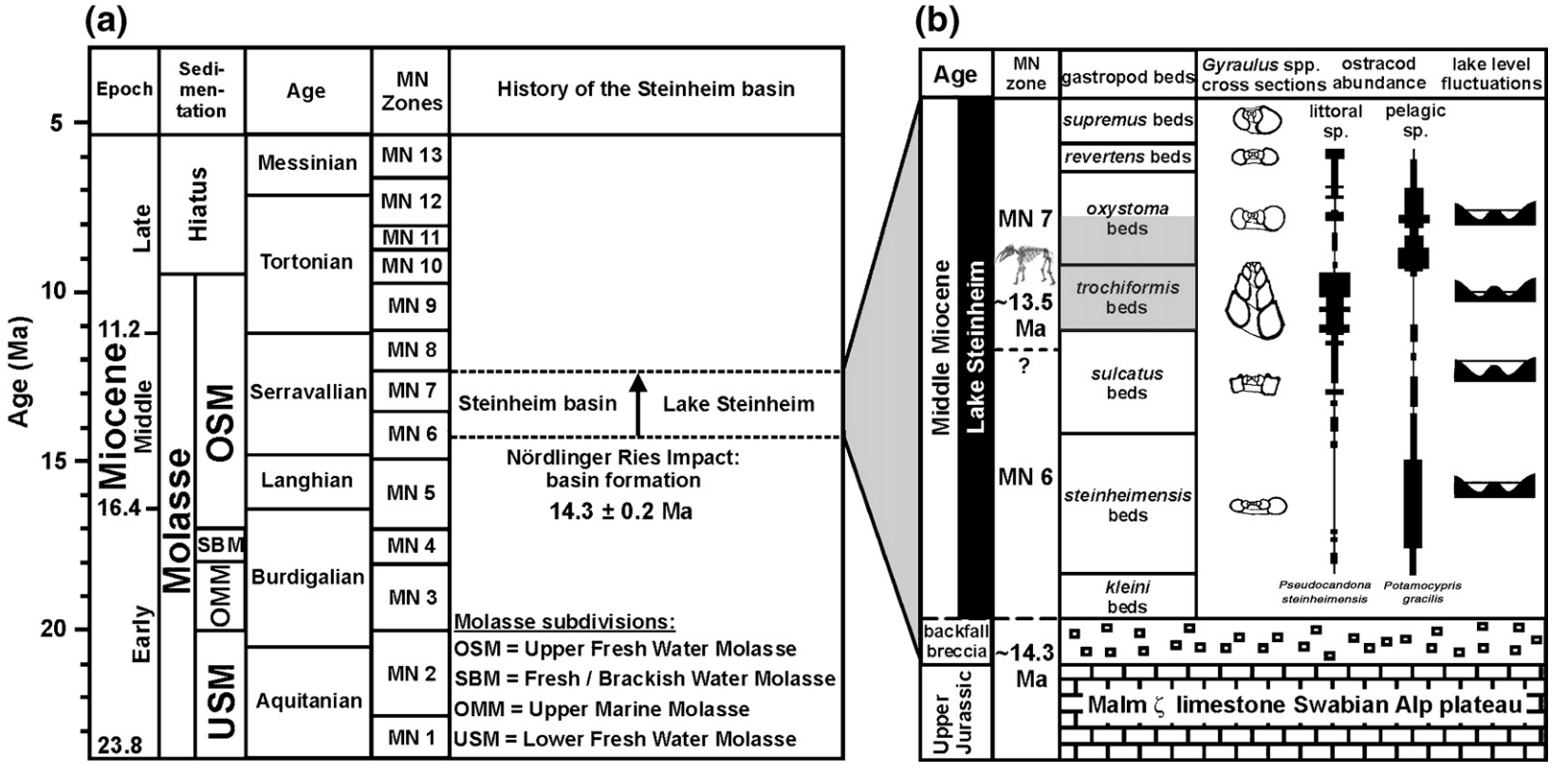

Fig. 2. a. The Steinheim basin craters formed contemporaneous with the Nördlinger Ries (Reiff, 1988), for which newest $^{39}Ar/^{40}Ar$ dates of impact glasses give an age of 14.3±0.2 Ma (Buchner et al., 2003). The abundant mammal remains date the Steinheim basin lake deposits biostratigraphically to the Middle Miocene European Neogene mammal zone MN 7 for which it is the reference locality (Heizmann and Reiff, 2002 and refs therein). MN zones are after Steininger (1999). The Miocene ages are after Berggren et al. (1995). b. Schematic stratigraphy of the lake sediments with the succession of the 7 different *Gyraulus* gastropod beds which form a calcareous sedimentary sequence of about 30 m thickness. The *Gyraulus* gastropods allow for a biostratigraphic classification of the otherwise lithostratigraphically uniform lake sediments. Typical cross sections of the different *Gyraulus* spp. are from Mensink (1984). Only the sediments of the *trochiformis* and lower *oxystoma* beds (grey shaded) contain mammal remains and were deposited during the lake level low-stand phase. The schematic lake level fluctuations and the associated abundance changes of two facies indicating ostracod species are drawn after Janz (1998).

layers. However, lake sediments can be biostratigraphically subdivided into distinct sedimentary units of gastropod beds, named after the 7 morphospecies of the planorbid freshwater gastropod *Gyraulus* spp. (*G. kleini*, *G. steinheimensis*, *G. sulcatus*, *G. trochiformis*, *G. oxystoma*, *G. revertens*, *G. supremus*) (Fig. 2b and photographs in Fig. 4). Lake Steinheim reached a maximum water depth of 120–160 m during the lake level high-stand of the *sulcatus* period. The lake became meromictic and oxygen deficient conditions existed in the deeper parts at this stage (Janz, 1992), resulting in the deposition of organic-rich leaf and fish layers (Weiler, 1934; Gaudant, 1989; Schweigert, 1993). During the *trochiformis* period the lake level decreased significantly reaching the low-stand in the upper *trochiformis*/lower *oxystoma* period (Mensink, 1984; Bahrig et al., 1986; Fig. 2). Mammal remains were mainly found in sediments from the slope of the central hill deposited during the lake level low-stand phase (Fig. 2b). Despite these fluctuations the lake never dried out until the end of the *supremus* period when the whole basin presumably was filled up with lake sediment (Bahrig et al., 1986). The thickness of the lake sediments is 30–40 m (Reiff, 1976); a continuous succession of the sediments has not been preserved due to Quaternary fluvial erosion.

2.3. Fossil fauna and flora of the Steinheim basin

About 230 animal and 90 plant species are represented as fossils within the lake sediments, making this locality one of the most important Miocene fossil localities in Europe with 54 preserved mammal taxa (Heizmann and Reiff, 2002). The faunal associations and especially the cricetids allow the Steinheim deposits to be placed into the European Neogene mammal assemblage zone MN 7 (Fahlbusch, 1976; Heissig, 1995), for which the deposits are also the reference locality (Steininger, 1999). The mammal fauna of Steinheim is a mixed fauna with woodland-related forms (*Palaeomeryx*, *Taucanamo*, *Heteroprox*, *Anchitherium*, *Hemicyon*), open, more arid landscape related forms (*Euprox* and *Listriodon*), probably representing faunal elements of a warm-temperate open landscape, and semi-aquatic species (*Stenofiber*, *Paralutra, Trochotherium)* (Heizmann, 1973; Heizmann and Reiff, 2002). Besides the large mammal fauna, small mammal remains are also found. The pika *P. oeningensis* is by far the most abundant mammal in Steinheim (Heizmann and Reiff, 2002).

During the lake level low-stand phase of the *trochiformis* period the central hill was exposed forming an island where the vertebrate carcasses probably accumulated by wind drift in shallow waters of the swampy littoral zone (Heizmann, 1973). The mammal remains are autochthonous and some of them are even articulated indicating that the animals died in/at the lake (Heizmann, 1973). Small mammal remains may also have been brought in by birds of prey (e.g., Heizmann, 1973; Heizmann and Fahlbusch, 1983; Heizmann and Reiff, 2002). Apart from mammal remains, further skeletal remains from other vertebrates such as birds, turtles, fish, and other taxa were found (Weiler, 1934; Mlynarski, 1980; Gaudant, 1989; Heizmann and Hesse, 1995; Heizmann and Reiff, 2002). The aquatic vertebrate fauna is not species-rich. *Tinca micropygoptera* is the predominant fish species well-adapted to standing water with muddy grounds and even oxygen-deficient conditions while the rare *Barbus steinheimensis* prefers well oxygenated flowing water and the skeletal remains are thought to have been brought in from an inflowing little creek (Weiler, 1934; Gaudant, 1989) but no geological indication for such a stretch of running water exists. The dominant turtle species of Steinheim *Chelydropsis murchisoni* was a fish-eating aquatic turtle while the herbivorous *Clemmydopsis turnauensis* was feeding on aquatic plants (Mlynarski, 1980). In contrast, otherwise abundant crocodiles were not found in the Steinheim basin (Schleich, 1985), probably because the isolated basin was not connected to the river network.

The lake sediments also contain a well-preserved invertebrate fauna with more than 100 gastropod and 53 ostracod species (Hilgendorf, 1866; Mensink, 1984; Gorthner, 1992; Janz, 1992, 1997, Finger, 1998; Heizmann and Reiff, 2002). The Steinheim basin is well-known for the intra-lacustrine speciation of the freshwater gastropod *Gyraulus* into distinct morphospecies, (Hilgendorf, 1866; Mensink, 1984; Gorthner, 1992), representing one of the earliest palaeontological examples for Darwin's evolution theory (Janz, 1999). A similar evolutionary pattern with morphological changes and one intra-lacustrine speciation is also known for the sympatric ostracods (Janz, 2000). Of the mostly non-endemic freshwater ostracods the benthic ostracod *Ilyocypris binocularis* is the most abundant species, occurring throughout the whole section of the lake sediments (Janz, 1992, 1997, 2000).

Charophyte remains are abundant in the lake sediments mostly as aragonitic mineralised stem fragments (Gregor, 1983, see also Fig. 3e) while gyrogonites are rare and only found in the basal lake sediments of the *kleini* beds (Schudack and Janz, 1997). The hydrophytes such as *Isoetes* and Characeae are characteristic for an oligotrophic lake setting (Schweigert, 1993). Floral

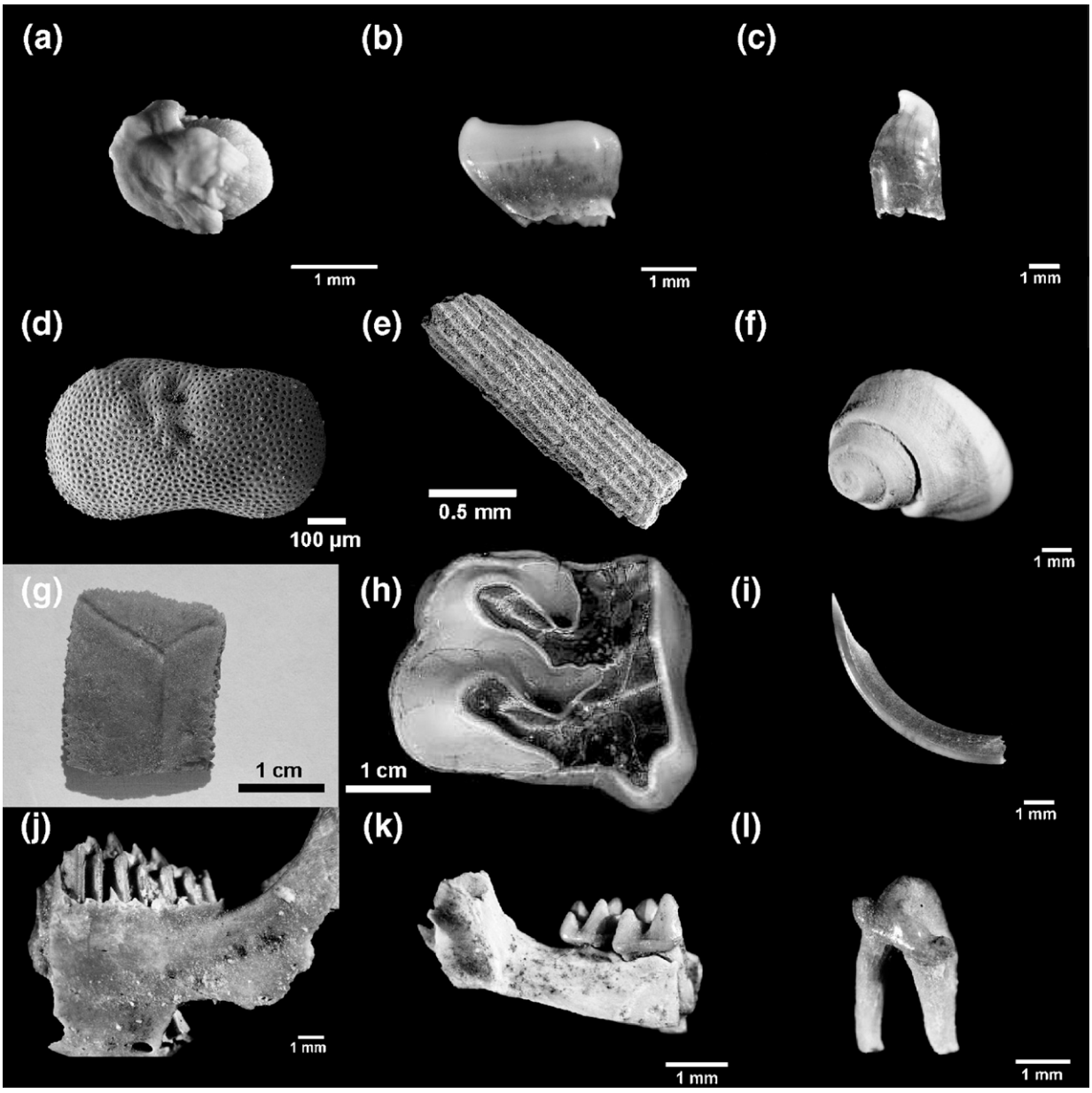

Fig. 3. Skeletal elements from vertebrates and invertebrates analysed for their isotopic compositions: (a) fish otolith: *T. micropygoptera*, (b) fish tooth: *T. micropygoptera*, (c) fish tooth: *B. steinheimensis*, (d) ostracod valve: *I. binocularis* (SEM picture), (e) characean fragment (SEM picture), (f) freshwater gastropod: *Gyraulus trochiformis*, (g) freshwater turtle carapace fragment: *Clemmydopsis* sp., (h) rhinoceros tooth: *Brachypotherium* sp., (i) incisor rodent indet., (j) Pika jaw: *P. oeningensis*, (k) hairy hedgehog jaw with two molars: *G. socialis*, (l) hairy hedgehog tooth: *G. socialis*.

remains preserved as impressions in the leaf layers indicate that the background vegetation around the Steinheim basin was a deciduous dry forest of Mediterranean-type with *Quercus*, accompanied by *Celtis*, *Juglans*, *Pistacia* and Leguminosae, species which are taken to be characteristic for a warm-temperate climate with a pronounced dry season (Schweigert, 1993). The lake shore, however, was surrounded by a humid alluvial forest (Gregor, 1983; Schweigert, 1993).

3. Material and methods

Phosphatic and carbonaceous fossil skeletal remains (Fig. 3) from Steinheim lake sediments have been analysed for their C, O, and Sr isotopic compositions

(Tables 1–13). All vertebrate skeletal remains originate from the former Pharion´s sand pit at the SW slope of the central hill and mammal remains come from the *trochiformis*/lower *oxystoma* gastropod beds (Fig. 2b), which is the only section of the lake profile with abundant mammal remains (Heizmann, 1973).

Tooth enamel samples from different large mammal taxa (proboscideans, rhinocerotids, equids, cervids, suids, and palaeomerycids) as well as whole teeth of sympatric small mammal taxa (pikas, hairy hedgehogs, and rodents) have been analysed. If available mammal teeth that formed late during ontogenesis, such as third molars, were chosen to avoid the influence of nursing on the isotopic composition of the body fluids. Enamel was sampled with a small diamond-studded drill over the whole enamel length from the crown to the root to get a representative mean sample of the period of tooth enamel formation. Depending on mammal species, tooth position, and enamel maturation the C, O, and Sr isotopic composition of tooth enamel from large mammals reflects the isotopic composition of food and water ingested during a period of >6 months up to

Table 1
O and C isotopic compositions of large mammal teeth

Sample	Species	Tooth	$\delta^{13}C$ [‰] VPDB	σ	$\delta^{18}O_{CO3}$ [‰] VPDB	σ	$\delta^{18}O_{CO3}$ [‰] VSMOW	CO3 [wt.%]	$\delta^{18}O_{PO4}$ [‰] VSMOW	σ
FZ RH ST 1	*Lartetotherium sansaniense*	Molar	−10.5	0.08	−7.9	0.11	22.7	3.9	18.6	0.3
FZ RH ST 2	*Dicerorhinus steinheimensis*	M3	−11.6	0.05	−5.7	0.08	25.0	5.3	20.1	0.3
FZ RH ST 3	*Brachypotherium brachypus*	Incisor	−13.7	0.04	−9.5	0.10	21.1	4.7	16.5	0.0
FZ RH ST 4	*Brachypotherium brachypus*	Molar	−12.8	0.04	−6.9	0.09	23.8	3.8		
FZ RH ST 5	*Brachypotherium brachypus*	Pd3	−13.1	0.07	−8.3	0.13	22.4	4.1	16.4	0.3
FZ RH ST 6	*Brachypotherium brachypus*	Canine	−12.9	0.06	−4.1	0.10	26.7	5.1	18.2	0.3
FZ RH ST 7	*Alicornops simorrense*	M3	−11.8	0.04	−7.7	0.10	23.0	3.3	17.7	0.3
FZ RH ST 8	*Brachypotherium brachypus*	P2	−12.1	0.08	−7.5	0.12	23.2	4.0	17.2	0.1
FZ RH ST 9	*Lartetotherium sansaniense*	M2	−10.6	0.07	−5.7	0.13	25.1	3.6	18.4	0.0
FZ RH ST 10	*Lartetotherium sansaniense*	M1	−12.8	0.09	−5.5	0.12	25.3	4.4		
FZ RH ST 11	*Lartetotherium sansaniense*	Molar	−11.5	0.07	−4.5	0.08	26.3	5.4	18.8	0.2
FZ RH ST 12	*Lartetotherium sansaniense*	Molar	−10.5	0.06	−6.0	0.09	24.7	6.1	17.3	0.2
FZ RH ST 13	*Aceratherium simorense*	Molar	−11.5	0.07	−6.2	0.09	24.5	3.1	18.4	0.2
FZ EQ ST 1	*Anchitherium aurelianense*	Molar	−9.9	0.05	−7.0	0.10	23.7	4.5		
FZ EQ ST 2	*Anchitherium aurelianense*	Molar	−12.3	0.08	−8.5	0.14	22.2	4.5	18.2	0.1
FZ EQ ST 3	*Anchitherium aurelianense*	molar	−10.0	0.08	−5.6	0.15	25.2	6.0	18.5	0.2
FZ EQ ST 4	*Anchitherium aurelianense*	Molar	−11.1	0.15	−6.6	0.18	24.1	4.9	17.1	0.2
FZ EQ ST 5	*Anchitherium aurelianense*	Molar	−11.8	0.05	−4.8	0.12	26.0	3.8	19.4	0.4
FZ EQ ST 6	*Anchitherium aurelianense*	Molar	−10.0	0.07	−5.2	0.12	25.6	3.9	19.1	0.1
FZ EQ ST 7	*Anchitherium aurelianense*	Molar	−10.8	0.03	−6.9	0.10	23.8	3.8	16.6	0.0
FZ CE ST 3	*Euprox od. Heteroprox*	Molar	−8.9	0.03	−1.9	0.08	29.0	6.9	21.6	0.1
FZ CE ST 4	*Euprox od. Heteroprox*	Premolar	−10.4	0.10	−3.4	0.16	27.4	4.1	20.2	0.1
FZ CE ST 5	*Euprox od. Heteroprox*	Molar	−10.3	0.04	−6.0	0.10	24.7	5.4	16.4	0.2
FZ CE ST 8	*Micromeryx flourensianus*	Molar	−10.2	0.05	−5.4	0.09	25.3	6.2	15.9	0.2
FZ CE ST 9	*Micromeryx flourensianus*	Molar	−10.0	0.06	−5.2	0.07	25.6	6.5	16.5	0.3
FZ CE ST 13	*Euprox od. Heteroprox*	M2	−10.9	0.02	−4.4	0.10	26.4	5.3	19.2	0.4
FZ CE ST 14	*cervid indet.*	Molar	−10.5	0.06	−1.8	0.14	29.0	7.3		
FZ CE ST 15	*cervid indet.*	Molar	−11.5	0.08	−6.7	0.14	24.0	5.1		
FZ CE ST 16	*cervid indet.*	Molar	−10.8	0.08	−3.9	0.11	26.9	4.5		
FZ PA ST 1	*Palaeomeryx eminens*	molar	−12.2	0.07	−2.3	0.11	28.5	4.3	23.6	0.3
FZ PA ST 2	*Palaeomeryx eminens*	Molar	−10.3	0.07	−2.5	0.10	28.3	4.3	24.0	0.1
FZ MA ST 1	*Gomphotherium steinheimense*	M3	−10.1	0.09	−6.3	0.19	24.4	6.4	17.3	0.0
FZ MA ST 2	*Gomphotherium steinheimense*	M3	−10.3	0.14	−7.7	0.17	22.9	4.9		
FZ MA ST 3	*Gomphotherium steinheimense*	Molar	−10.7	0.06	−7.8	0.10	22.9	5.7	16.8	0.2
FZ SU ST 1	*Conohyus simorrensis*	M3	−10.8	0.09	−7.0	0.14	23.7	5.0	17.2	0.3
FZ SU ST 2	*Conohyus simorrensis*	M2	−10.3	0.16	−7.4	0.11	23.3	4.5	17.6	0.2
FZ SU ST 3	*Conohyus simorrensis*	M3	−10.3	0.09	−8.6	0.16	22.0	5.7	15.3	0.3
FZ SU ST 4	*Albanohyus pygmaeus*	Molar	−10.0	0.06	−3.3	0.07	27.5	5.8	20.1	0.2
FZ SU ST 5	*Conohyus simorrensis*	Molar	−10.5	0.06	−5.9	0.14	24.8	2.5	19.8	0.2
FZ SU ST 6	*Listriodon splendens*	Canine	−12.7	0.10	−4.5	0.15	26.2	5.7	20.4	0.3
FK TRO ST 1	*Trochotherium cyamoides*	Bone	−8.5	0.06	−2.7	0.11	28.2	8.3	20.4	0.2

Table 2
O and C isotopic compositions of small mammal teeth

Sample	Species	Tooth	$\delta^{13}C$ [‰] VPDB	σ	$\delta^{18}O_{CO3}$ [‰] VPDB	σ	$\delta^{18}O_{CO3}$ [‰] VSMOW	CO3 [wt.%]	$\delta^{18}O_{PO4}$ [‰] VSMOW	σ
FK GA ST 2	*Galerix socialis*	Jaw bone	−8.6	0.07	−2.0	0.09	28.9	9.6	21.7	0.1
FZ GA ST 3	*Galerix socialis*	Molar	−8.1	0.05	−4.0	0.08	26.8	8.6	22.0	0.1
FK GA ST 3	*Galerix socialis*	Jaw bone	−8.0	0.05	−3.5	0.07	27.3	9.6	20.7	0.9
FZ GA ST 4	*Galerix socialis*	Molar							20.0	0.0
FZ RO ST 2	*Rodent indet.*	Incisor	−8.7	0.13	−1.5	0.11	29.3	7.4	24.9	0.3
FZ RO ST 3	*Rodent indet.*	Incisor	−9.7	0.05	−3.5	0.08	27.3	6.8	16.8	0.2
FZ RO ST 4	*Rodent indet.*	Incisor	−8.4	0.03	−3.2	0.08	27.7	8.8	21.1	0.1
FZ RO ST 5	*Rodent indet.*	Incisor	−8.2	0.06	−2.6	0.07	28.3	9.4	20.7	0.1
FZ RO ST 6	*Rodent indet.*	Incisor	−8.6	0.03	−2.4	0.06	28.5	7.0	24.3	0.8
FZ LA ST 1	*Prolagus oeningensiss*	Molar	−9.8	0.04	−3.7	0.09	27.0	7.0	19.4	0.5
FZ LA ST 2	*Prolagus oeningensis*	Molar	−9.1	0.05	−0.9	0.08	30.0	10.4	23.9	0.3
FZ LA ST 3	*Prolagus oeningensis*	Molar	−10.5	0.06	−5.6	0.12	25.2	8.3	16.8	0.4
FK LA ST 4	*Prolagus oeningensis*	Jaw bone	−8.6	0.05	−2.7	0.06	28.1	10.4	21.2	0.1
FZ LA ST 4	*Prolagus oeningensis*	Molar	−10.1	0.06	−5.1	0.11	25.7	8.8	17.8	0.1
FZ LA ST 5	*Prolagus oeningensis*	Molar	−9.9	0.04	−5.7	0.06	25.0		15.9	0.3
FZ LA ST 6	*Prolagus oeningensis*	Molar	−8.8	0.04	−1.9	0.08	29.0	8.2	22.8	0.3
FZ LA ST 7	*Prolagus oeningensis*	Molar	−9.8	0.05	−5.7	0.08	25.0	6.4	19.6	0.2

2 years (e.g., Hillson, 2005; Hoppe et al., 2004; Kohn, 2004) whereas in small mammal teeth only shorter time periods of only a few weeks or months are recorded (e.g., Lindars et al., 2001 and references therein).

Powdered whole teeth of two fish species (*T. micropygoptera*, *B. steinheimensis*) were analysed from the mammal-bearing sediments and *Tinca* teeth also from the fish layer in the *sulcatus* gastropod bed (Table 3). Furthermore, teeth of *Palaeoleuciscus* sp., occurring only in the *kleini* beds, were analysed.

Aragonitic shells of the freshwater gastropod *Gyraulus* spp. and sympatric calcitic valves of the benthic ostracod *I. binocularis*, which both occur over the whole stratigraphic range of the lake sediment sequence, were analysed from 43 samples covering all seven gastropod beds (Fig. 4, Tables 9 and 10). The ostracods and

Table 3
O and C isotopic composition of fish teeth

Sample	Species	Gastropod bed	Skeletal element	$\delta^{13}C$ [‰] VPDB	σ	$\delta^{18}O_{CO3}$ [‰] VPDB	σ	$\delta^{18}O_{CO3}$ [‰] VSMOW	CO3 [wt.%]	$\delta^{18}O_{PO4}$ [‰] VSMOW	σ
FZ SL ST 1	*Tinca micropygoptera*	*trochiformis/oxystoma*	Tooth	−6.5	0.11	−1.4	0.12	29.5	6.8	23.0	0.2
FZ SL ST 2	*Tinca micropygoptera*	*trochiformis/oxystoma*	Tooth	−7.2	0.07	−1.8	0.11	29.1	6.7	24.1	0.3
FZ SL ST 3	*Tinca micropygoptera*	*trochiformis/oxystoma*	Tooth	−5.7	0.09	−1.7	0.10	29.2	3.8		
FZ SL ST 4	*Tinca micropygoptera*	*trochiformis/oxystoma*	Tooth	−5.9	0.12	−1.9	0.14	29.0	4.5		
FZ SL ST 5	*Tinca micropygoptera*	*trochiformis/oxystoma*	Tooth	−6.0	0.07	−1.9	0.15	29.0	4.2		
FZ SL ST 6	*Tinca micropygoptera*	*trochiformis/oxystoma*	Tooth	−6.6	0.05	−1.7	0.07	29.1	8.4	24.5	0.1
FZ SL ST 7	*Tinca micropygoptera*	*trochiformis/oxystoma*	Tooth	−6.3	0.04	−1.9	0.06	28.9	8.2	24.2	0.6
FZ SL ST 10	*Tinca micropygoptera*	*trochiformis/oxystoma*	Tooth	−6.6	0.05	−2.4	0.07	28.4	9.8		
FZ SL ST 11	*Tinca micropygoptera*	*sulcatus* (fish layer)	Tooth	−7.5	0.07	−1.7	0.11	29.2	3.7		
FZ SL ST 13	*Tinca micropygoptera*	*sulcatus* (fish layer)	Tooth	−6.9	0.05	−2.5	0.09	28.4	3.5		
FZ SL ST FI	*Tinca micropygoptera*	*sulcatus* (fish layer)	11 teeth	−7.5	0.06	−1.1	0.07	29.8	7.5	23.9	0.3
FZ BA ST 1	*Barbus steinheimensis*	*trochiformis/oxystoma*	Tooth	−5.9	0.06	−1.3	0.09	29.5	6.2	24.2	0.3
FZ BA ST 2	*Barbus steinheimensis*	*trochiformis/oxystoma*	Tooth	−5.8	0.07	−1.7	0.07	29.2	7.4	24.1	0.0
FZ BA ST 3	*Barbus steinheimensis*	*trochiformis/oxystoma*	Tooth	−6.0	0.07	−1.2	0.07	29.6	6.0	25.3	0.8
FZ BA ST 4	*Barbus steinheimensis*	*trochiformis/oxystoma*	Tooth	−5.8	0.08	−1.8	0.22	29.1	6.8		
FZ BA ST 5	*Barbus steinheimensis*	*trochiformis/oxystoma*	Tooth	−6.6	0.09	−2.3	0.11	28.5	6.2		
FZ BA ST 6	*Barbus steinheimensis*	*trochiformis/oxystoma*	Tooth	−6.9	0.05	−1.7	0.06	29.2	8.3	25.7	0.2
FK BA ST 8	*Barbus steinheimensis*	*kleini*	Bone							22.8	0.0
FZ PA ST 1	*Palaeoleuciscus*	*kleini*	3 teeth	−2.4	0.09	−4.1	0.08	26.6	14.2	17.8	

Table 4
O and C isotopic compositions of turtle bones

Sample	Species	Gastropod bed	Skeletal element	$\delta^{13}C$ [‰] VPDB	σ	$\delta^{18}O_{CO3}$ [‰] VPDB	σ	$\delta^{18}O_{CO3}$ [‰] VSMOW	CO3 [wt.%]	$\delta^{18}O_{PO4}$ [‰] VSMOW	σ
FK SCH ST 1	*Testudo* sp.	*trochiformis/oxystoma*	Carapace	−8.2	0.06	−1.0	0.10	29.9	9.5		
FK SCH ST 2	*Testudo* sp.	*trochiformis/oxystoma*	Carapace	−8.2	0.05	−0.7	0.05	30.2	10.2		
FK SCH ST 7	*Chelydropsis murchisoni*	*trochiformis/oxystoma*	Carapace	−8.3	0.05	−1.8	0.09	29.1	11.6		
FK SCH ST 8	*Chelydropsis murchisoni*	*trochiformis/oxystoma*	Carapace	−8.4	0.07	−1.5	0.11	29.4	10.7	24.6	
FK SCH ST 9	*Chelydropsis murchisoni*	*trochiformis/oxystoma*	Carapace	−8.3	0.07	−1.8	0.12	29.1	10.9	23.4	0.1
FK SCH ST 10	*Chelydropsis murchisoni*	*trochiformis/oxystoma*	Carapace	−8.3	0.07	−2.1	0.10	28.7	11.5	24.4	0.3
FK SCH ST 11	*Chelydropsis murchisoni*	*trochiformis/oxystoma*	Carapace	−8.2	0.06	−2.4	0.10	28.4	12.7		
FK SCH ST 12	*Chelydropsis murchisoni*	*trochiformis/oxystoma*	Carapace	−8.1	0.06	−2.0	0.09	28.8	10.6		
FK SCH ST 13	*Clemmydopsis turnauensis*	*trochiformis/oxystoma*	Carapace	−8.2	0.04	−0.6	0.08	30.3	9.6	24.1	0.1
FK SCH ST 14	*Clemmydopsis turnauensis*	*trochiformis/oxystoma*	Carapace	−8.0	0.09	−1.5	0.10	29.4	8.8	24.2	0.1
FK SCH ST 15	*Clemmydopsis turnauensis*	*trochiformis/oxystoma*	Carapace	−8.4	0.08	−0.7	0.10	30.2	7.1	23.8	0.2

freshwater gastropods originate from several sediment sections and outcrops in the Steinheim basin forming a combined sediment profile of about 30 m thickness (Janz, 1992, 1997, 2000).

In the *kleini* and *steinheimensis* beds where *I. binocularis* is not as abundant, additional specimens of *Ilyocypris* sp. were analysed. Only clean and transparent valves of adult individuals were chosen for isotopic analysis. The gastropod shells were cleaned from adhering sediment in distilled water using ultrasonification. The best preserved gastropod shells were selected, carefully crushed and sediment fillings or shell fragments with carbonate overgrowth were removed under a binocular microscope. The chosen fragments were powdered and homogenized in an agate mortar. 50 samples from all 7 *Gyraulus* spp. have been analysed by X-ray diffraction and all, except for two that contained some secondary calcite (Ph 12-2 and S 35-3), still consisted of pure aragonite (>95 wt.%).

Fish teeth and otoliths from *T. micropygoptera* as well as charophyte stem fragments and carbonate sediment particles were hand-picked from a sediment sample of the fish layer from the *sulcatus* beds and analysed for their C and O isotopic composition (Tables 5–7).

3.1. C and O isotope measurements of the carbonate in the phosphate and carbonate

Tooth enamel and bone powders were chemically pre-treated with 2% NaOCl solution, followed by a 1 M Ca-acetate acetic acid buffer solution (Koch et al., 1997), prior to analysis of the carbon ($\delta^{13}C$) and oxygen ($\delta^{18}O_{CO3}$) isotopic composition of the carbonate in the phosphate, the oxygen isotopic composition of the phosphate ($\delta^{18}O_{PO4}$), and the strontium isotopic composition ($^{87}Sr/^{86}Sr$).

For C and O isotopic analysis of the carbonate in the phosphate of bone and teeth about 3 mg was used. For carbonate analysis 200 μg (gastropod shells) or 30 to 80 μg (ostracod valves) was used. Commonly between 2 and 4 ostracod valves were assembled for a single isotope measurement. The samples were analysed at 70 °C using a ThermoFinnigan Gasbench II on a Finnigan Delta Plus XL continuous flow isotope ratio gas mass spectrometer at the University of Lausanne, following a procedure adapted after Spötl and Vennemann (2003). The measured carbon and oxygen isotopic compositions were normalized to the in-house Carrara marble calcite standard that has been calibrated against

Table 5
O and C isotopic composition of characean stem fragments

Sample	Material	Gastropod bed	Profile (m)	$\delta^{13}C$ [‰] VPDB	σ	$\delta^{18}O_{CO3}$ [‰] VPDB	σ	$\delta^{18}O_{CO3}$ [‰] VSMOW	CO3 [wt.%]
CHA ST 1	*Characea indet*	*sulcatus* (fish layer)	16	4.4	0.03	2.7	0.05	33.7	95.3
CHA ST 2	*Characea indet*	*sulcatus* (fish layer)	16	3.7	0.06	4.4	0.07	35.5	93.1
CHA ST 3	*Characea indet*	*sulcatus* (fish layer)	16	3.4	0.05	2.4	0.07	33.4	84.0
CHA ST 4	*Characea indet*	*sulcatus* (fish layer)	16	3.6	0.07	3.9	0.07	35.0	88.6
CHA ST 5	*Characea indet*	*sulcatus* (fish layer)	16	3.9	0.04	2.5	0.09	33.5	102.8
CHA ST 6	*Characea indet*	*sulcatus* (fish layer)	16	3.1	0.08	4.8	0.08	35.9	91.0

Table 6
O and C isotopic compositions of carbonaceaous sediment particles

Sample	Material	Gastropod bed	Profile (m)	$\delta^{13}C$ [‰]	σ	$\delta^{18}O_{CO3}$ [‰] VPDB	σ	$\delta^{18}O_{CO3}$ [‰] VSMOW	CO3 [wt.%]
SED ST 1	Carbonate sediment	*sulcatus* (fish layer)	16	3.9	0.05	3.6	0.07	34.6	104.5
SED ST 2	Carbonate sediment	*sulcatus* (fish layer)	16	3.4	0.05	1.1	0.07	32.1	104.2
SED ST 3	Carbonate sediment	*sulcatus* (fish layer)	16	4.3	0.07	2.7	0.14	33.7	86.6
SED ST 4	Carbonate sediment	*sulcatus* (fish layer)	16	3.7	0.08	4.2	0.09	35.2	86.2
SED ST 5	Carbonate sediment	*sulcatus* (fish layer)	16	2.1	0.06	0.9	0.09	31.9	88.6
SED ST 6	Carbonate sediment	*sulcatus* (fish layer)	16	3.5	0.06	2.3	0.07	33.3	85.6

NBS-19 and reported in the usual δ-notation vs. VPDB. The normalization incorporates the CO_2-carbonate acid fractionation factor for calcite, both for the calcite samples analysed as well as the carbonate in phosphate. $\delta^{18}O$ values for aragonite samples have not been corrected relative to the normalization against calcite. External reproducibility for carbonate in the phosphate was checked with pre-treated NBS 120c Florida phosphate rock standard giving values of $\delta^{13}C_{VPDB} = -6.29 \pm 0.08$‰ and $\delta^{18}O_{VPDB} = -2.32 \pm 0.14$‰ ($n = 13$). The external reproducibility for the carbon and oxygen isotopic composition of carbonate in the phosphate is better than ±0.1‰ and ±0.15‰, respectively. For pure carbonate samples the reproducibility was better than ±0.1‰ for both carbon and oxygen isotope measurements.

3.2. O isotope measurements of the phosphate using TC-EA

Oxygen isotope composition of phosphate ($\delta^{18}O_{PO4}$) was measured on about 4 mg of pre-treated powder precipitated as silver phosphate (Ag_3PO_4) according to a method modified after Dettmann et al. (2001). Samples were dissolved in 800 µl 2 M HF in a 2 ml safe lock centrifuge tube over night. The centrifuged solution was transferred into a new 2 ml centrifuge tube leaving the CaF residue behind. The HF was neutralized by addition of 140 µl of 25% NH_4OH solution and the dissolved phosphate precipitated as Ag_3PO_4 by the addition of 800 µl of a 2 M $AgNO_3$ solution. The Ag_3PO_4 precipitate was washed two times with distilled water and oven-dried at 50 °C. The Ag_3PO_4 yields were monitored for each sample and gave in the mean 2.1±0.1 mg Ag_3PO_4 for 1.0 mg of enamel powder. Ag_3PO_4 of each sample and standard was analysed in triplicate for its oxygen isotopic composition according to methods described in Vennemann et al. (2002) using a TC-EA at 1450 °C linked to a ThermoFinnigan Delta Plus XL gas mass spectrometer at the University of Lausanne. Several isotopically distinct standards (TU 1, TU 2, benzoic acid, K_2HPO_4, NBS 120c), which cover the range of oxygen isotopic compositions of the analysed samples, were measured and used for off-line normalization (Vennemann et al., 2002). $\delta^{18}O_{PO4}$ values are reported

Table 7
O and C isotopic compositions of fish otoliths (*Tinca micropygoptera*)

Sample	Material	Gastropod bed	Profile (m)	$\delta^{13}C$ [‰] VPDB	σ	$\delta^{18}O_{CO3}$ [‰] VPDB	σ	$\delta^{18}O_{CO3}$ [‰] VSMOW	CO3 [wt.%]
OT SL ST 1	Otolith	*sulcatus* (fish layer)	16	−12.4	0.07	1.1	0.07	32.1	65.2
OT SL ST 3	Otolith	*sulcatus* (fish layer)	16	−11.5	0.07	1.1	0.07	32.0	64.9
OT SL ST 4	Otolith	*sulcatus* (fish layer)	16	−12.8	0.07	0.8	0.07	31.7	65.1
OT SL ST 5	Otolith	*sulcatus* (fish layer)	16	−11.7	0.05	0.9	0.07	31.9	70.1
OT SL ST 7	Otolith	*sulcatus* (fish layer)	16	−12.2	0.05	1.0	0.05	32.0	63.3
OT SL ST 8	Otolith	*sulcatus* (fish layer)	16	−12.6	0.07	1.2	0.08	32.1	62.5
OT SL ST 10	Otolith	*sulcatus* (fish layer)	16	−11.6	0.06	0.6	0.07	31.6	72.6
OT SL ST 11	Otolith	*sulcatus* (fish layer)	16	−11.4	0.06	0.5	0.04	31.4	62.0
OT SL ST 12	Otolith	*sulcatus* (fish layer)	16	−9.5	0.05	1.0	0.09	32.0	76.9
OT SL ST 13	Otolith	*sulcatus* (fish layer)	16	−13.0	0.04	1.5	0.05	32.5	59.7
OT SL ST 15	Otolith	*sulcatus* (fish layer)	16	−11.2	0.09	1.2	0.07	32.2	68.3
OT FI ST 1	Otolith	*kleini*	0.5	−9.9	0.06	−5.2	0.10	25.5	90.6

Table 8
O and C isotopic compositions of bivalves and ostracods from other Miocene localities

Sample	Material	Locality	$\delta^{13}C$ [‰]	σ	$\delta^{18}O_{CO3}$ [‰] VPDB	σ	$\delta^{18}O_{CO3}$ [‰] VSMOW	CO3 [wt.%]
MU HE 1	*Unionidae* fresh water bivalve	Helsighausen, Switzerland	−6.1	0.06	−10.4	0.12	20.2	91.0
MU HE 2	*Unionidae* fresh water bivalve	Helsighausen, Switzerland	−6.2	0.05	−10.6	0.13	20.0	94.6
MU HE 3	*Unionidae* fresh water bivalve	Helsighausen, Switzerland	−6.2	0.05	−10.6	0.09	20.0	93.8
MU HE 4	*Unionidae* fresh water bivalve	Helsighausen, Switzerland	−6.1	0.07	−9.9	0.09	20.7	99.9
MU HE 5	*Unionidae* fresh water bivalve	Helsighausen, Switzerland	−6.0	0.06	−10.1	0.08	20.5	95.0
MU HUE 1	*Unionidae* fresh water bivalve	Hülistein, Switzerland	−4.2	0.05	−9.8	0.08	20.8	88.2
MU HUE 2	*Unionidae* fresh water bivalve	Hülistein, Switzerland	−2.2	0.04	−9.4	0.07	21.2	86.4
GA HUE 1	*Unionidae* fresh water bivalve	Hülistein, Switzerland	−3.0	0.04	−9.5	0.05	21.2	79.3
OS HW 1	*Eucypris lutzae* ostracod	Höwenegg, Gemany	−7.1	0.07	−7.6	0.06	23.6	95.3
OS HW 2	*Eucypris lutzae* ostracod	Höwenegg, Gemany	−7.4	0.07	−7.7	0.05	23.3	93.4
OS HW 3	*Eucypris lutzae* ostracod	Höwenegg, Gemany	−7.2	0.07	−7.6	0.03	23.5	86.6
OS HW 4	*Eucypris lutzae* ostracod	Höwenegg, Gemany	−6.7	0.09	−9.1	0.09	24.1	65.7
OS HW 5	*Eucypris lutzae* ostracod	Höwenegg, Gemany	−7.3	0.05	−10.1	0.06	23.4	81.8
OS HW 6	*Eucypris lutzae* ostracod	Höwenegg, Gemany	−2.7	0.06	−0.6	0.05	28.1	83.9
OS NÖ 1	*Strandesia risgoviensis* ostracod	Nördlinger Ries, Germany	3.9	0.05	2.3	0.05	34.9	94.5
OS NÖ 2	*Strandesia risgoviensis* ostracod	Nördlinger Ries, Germany	3.4	0.06	1.6	0.04	34.4	102.7
OS NÖ 3	*Strandesia risgoviensis* ostracod	Nördlinger Ries, Germany	3.5	0.05	1.7	0.02	34.6	93.5

in the usual δ-notation vs. VSMOW. The Ag_3PO_4 precipitated from the NBS 120c standard analysed in different TC-EA runs gave a mean $\delta^{18}O_{PO4}$ value of 21.6±0.4‰, (n=25), a value similar to that published for this standards elsewhere (e.g., Strait et al., 2004).

3.3. Sr isotope measurements

The preparation for Sr isotopic analysis was done in a clean laboratory. A 1 mg aliquot of the pre-treated enamel powder used for stable isotope analysis or 1 mg of aragonite was dissolved in 1 ml distilled 7 N HNO_3, respectively 6 N HCl in Savillex® beakers over night. The Sr fraction was separated with standard separation procedure on quartz glass cation exchange columns filled with 5 ml resin bed of BioRad AG 50W-X12, 200–400 mesh using 2.5 N HCl. The purified Sr was taken up in 1 µl of 2.5 N HCl and loaded on tungsten filaments coated with 2×0.7 µl of TaF_5 activator. The Sr isotopic composition was measured with a Finnigan MAT 262 thermal ionization mass spectrometer (TIMS) at the University of Tübingen. For each sample >200 $^{87}Sr/^{86}Sr$ ratios were measured in the static mode with an internal precision $\leq 10\times10^{-6}$. $^{87}Sr/^{86}Sr$ ratios were corrected for mass fractionation in the instrument, using the natural $^{88}Sr/^{86}Sr$ ratio of 8.375209. Measured $^{87}Sr/^{86}Sr$ ratios were normalized to the certified value of NBS 987 ($^{87}Sr/^{86}Sr$=0.710248). The NBS 987 gave a mean $^{87}Sr/^{86}Sr$=0.710246±9, (n=7) during the period of Sr isotope measurements.

4. Results

Results for the stable isotope measurements of this study are given in Tables 1–10. Results for the Sr isotope compositions are given in Tables 11 to 12. Additional results for carbon isotopic compositions of dissolved inorganic carbon, oxygen isotopic composition of water ($\delta^{18}O_{H2O}$), and the Sr isotopic composition for some modern surface and groundwater samples from the Steinheim basin are given in Tables 13 and 15. In the following the range of isotope values for the different skeletal tissues are given followed by the mean value± standard deviation in brackets.

4.1. C and O isotope compositions of ostracod valves

Calcitic valves of the benthic ostracod *I. binocularis* have $\delta^{18}O$ values ranging from −2.3 to +4.0‰ ($\delta^{18}O$=+1.7±1.2‰, n=68) and $\delta^{13}C$ values between −4.0 and +1.9‰ ($\delta^{13}C$=−0.5±0.9‰, n=68) (Table 10). Samples of *Ilyocypris* sp. analysed from the lower lake sediments of the *steinheimensis* and *kleini* beds have similar $\delta^{13}C$ values but about 2‰ higher $\delta^{18}O$ values compared to *I. binocularis* from the same samples (Fig. 4). Lowest $\delta^{18}O$ and $\delta^{13}C$ values for both ostracod species occur in the basal lake sediments of the *kleini* beds.

4.2. C and O isotope compositions of gastropod shells

The $\delta^{18}O$ values of the aragonitic *Gyraulus* spp. shells range from −3.6 to +4.0‰ ($\delta^{18}O$=+2.0±1.3‰,

Table 9
O and C isotopic compositions gastropod shells (*Gyraulus* spp.)

Sample	Gastropod bed	Profile (m)	Shell weight (mg)	$\delta^{13}C$ [‰] VPDB	σ	$\delta^{18}O$ [‰] VPDB	σ	$\delta^{18}O$ [‰] VSMOW
SUP 1	*supremus*			−0.6	0.04	1.7	0.07	32.7
SUP 2	*supremus*			1.0	0.04	2.5	0.08	33.4
SUP 3	*supremus*			−1.7	0.05	1.1	0.09	32.1
SUP 4	*supremus*			−0.9	0.05	1.6	0.07	32.6
SUP 5	*supremus*			−1.4	0.04	2.2	0.07	33.2
K 19-2	*supremus*	22.4	8.7	−0.7	0.04	1.1	0.08	32.1
K 19-4	*supremus*	22.4	8.1	−0.3	0.13	3.9	0.16	34.9
REV 1	*revertens*			−1.5	0.05	0.8	0.07	31.8
REV 2	*revertens*			0.0	0.05	1.9	0.07	32.9
REV 3	*revertens*			−0.1	0.04	1.9	0.09	32.9
REV 4	*revertens*			0.1	0.04	2.0	0.05	33.0
REV 5	*revertens*			−2.1	0.03	3.3	0.08	34.3
K 14-2	*revertens*	21.5	0.5	1.0	0.08	2.5	0.12	33.5
K 14-3	*revertens*	21.5	0.4	1.3	0.06	2.2	0.12	33.2
K 8-2	*revertens*	20.4	3.7	1.5	0.09	1.9	0.13	32.9
K 8-3	*revertens*	20.4	1.8	0.0	0.07	2.5	0.09	33.5
K 5-1	*oxystoma*	20.15	6.7	−0.5	0.13	1.1	0.16	32.1
K 5-2	*oxystoma*	20.15	5.8	−1.2	0.09	1.0	0.12	32.0
K 1-1	*oxystoma*	19.6	4.7	−1.2	0.30	0.6	0.30	31.5
K 1-2	*oxystoma*	19.6	6.0	0.3	0.08	2.4	0.13	33.4
Ph 19-1	*oxystoma*	19.2	2.7	−1.2	0.08	0.6	0.11	31.5
Ph 19-3	*oxystoma*	19.2	1.7	−1.2	0.06	3.3	0.10	34.3
Ph 16-2	*oxystoma*	18.9	1.1	0.7	0.04	3.5	0.08	34.5
Ph 16-3	*oxystoma*	18.9	3.7	−0.7	0.05	1.1	0.09	32.1
Ph 12-1	*oxystoma*	18.3	2.4	−2.2	0.09	2.8	0.12	33.8
Ph 12-2	*oxystoma*	18.3	2.4	1.2	0.27	4.0	0.29	35.0
Ph 10-2	*oxystoma*	18	5.3	0.5	0.08	3.8	0.09	34.8
Ph 10-4	*oxystoma*	18	4.3	−0.4	0.07	3.1	0.12	34.1
Ph 8-1	*oxystoma*	17.7	3.0	−0.4	0.13	1.3	0.15	32.2
Ph 8-2	*oxystoma*	17.7	1.7	−0.5	0.10	2.8	0.11	33.8
Ph 6-1	*oxystoma*	17.4	4.1	−0.4	0.11	1.3	0.10	32.2
Ph 6-2	*oxystoma*	17.4	2.3	−1.1	0.11	1.2	0.07	32.2
Ph 4-1	*oxystoma*	17.1	5.2	0.5	0.07	0.9	0.12	31.9
Ph 4-2	*oxystoma*	17.1	3.9	−2.0	0.06	0.5	0.09	31.5
Ph 2-1	*oxystoma*	16.6	10.1	−1.3	0.06	2.0	0.08	33.0
Ph 2-2	*oxystoma*	16.6	8.4	−0.1	0.07	1.1	0.11	32.0
S 37-2	*oxystoma*	16.45	1.9	−2.5	0.05	2.5	0.11	33.5
S 37-3	*oxystoma*	16.45	1.6	−1.7	0.04	0.6	0.09	31.6
S 35-3	*oxystoma*	16.25	83.6	−0.7	0.09	2.9	0.10	33.8
S 33-2	*oxystoma*	15.6	46.4	−1.6	0.16	0.8	0.27	32.5
S 33-3	*oxystoma*	15.6	55.3	−1.2	0.03	1.6	0.03	32.5
S 31-1	*trochiformis*	15.2	53.7	−1.3	0.03	3.0	0.04	34.0
S 31-3	*trochiformis*	15.2	35.0	−0.7	0.05	1.4	0.07	32.4
S 27-1	*trochiformis*	14.65	66.	−0.6	0.03	1.4	0.07	32.3
S 27-3	*trochiformis*	14.65	38.5	−1.5	0.04	2.7	0.04	33.7
S 21-2	*trochiformis*	13.7	41.5	−0.6	0.03	2.7	0.07	33.7
S 21-3	*trochiformis*	13.7	37.8	0.1	0.05	2.0	0.06	33.0
S 18-1	*trochiformis*	13.3	48.3	−0.3	0.06	1.5	0.07	32.4
S 18-3	*trochiformis*	13.3	19.0	0.3	0.08	1.7	0.07	32.6
S 15-1	*trochiformis*	13.15	28.7	−0.1	0.07	1.0	0.08	31.9
S 15-3	*trochiformis*	13.15	22.3	−0.5	0.05	1.5	0.06	32.4
S 13-2	*trochiformis*	13	9.7	1.2	0.04	0.5	0.07	31.4
S 13-4	*trochiformis*	13	12.4	−0.2	0.07	0.3	0.08	31.2
S 10-1	*trochiformis*	12.75	27.8	−0.7	0.05	2.1	0.08	33.1
S 10-3	*sulcatus*	12.75	17.2	−0.3	0.10	1.3	0.10	32.2
SF 9-2	*sulcatus*	11.2	40.6	−1.0	0.09	3.5	0.12	34.5
SF 9-3	*sulcatus*	11.2	36.6	−0.5	0.13	4.0	0.18	35.0

Table 9 (*continued*)

Sample	Gastropod bed	Profile (m)	Shell weight (mg)	$\delta^{13}C$ [‰] VPDB	σ	$\delta^{18}O$ [‰] VPDB	σ	$\delta^{18}O$ [‰] VSMOW
S 1-1	*sulcatus*	10.75	13.1	−0.9	0.15	2.3	0.14	33.3
S 1-2	*sulcatus*	10.75	17.9	−1.2	0.05	1.6	0.07	32.6
SF 10-2	*sulcatus*	10.4	15.8	−0.2	0.07	1.0	0.09	31.9
SF 13-1	*sulcatus*	9.6	32.2	−1.8	0.06	1.6	0.09	32.5
SF 13-2	*sulcatus*	9.6	27.4	−1.5	0.04	2.7	0.09	33.7
SF 16-1	*sulcatus*	8.9	14.7	−1.0	0.05	1.5	0.06	32.4
SF 16-3	*sulcatus*	8.9	12.0	−0.9	0.05	0.6	0.07	31.5
SF 18-2	*sulcatus*	7.8	8.5	−1.2	0.05	1.6	0.08	32.5
B 25.1-1	*sulcatus*	6.85	20.2	−1.2	0.04	2.3	0.09	33.3
B 25.1-2	*sulcatus*	6.85	3.5	−2.0	0.06	3.5	0.10	34.6
B 26.9-1	*sulcatus*	5	4.5	−2.7	0.05	2.8	0.09	40.8
B 26.9-2	*sulcatus*	5	4.5	−1.9	0.06	3.4	0.07	41.4
B 28.1-1	*sulcatus*	3.9	24.5	−2.5	0.05	3.7	0.09	41.8
B 28.1-2	*sulcatus*	3.9	15.6	−1.3	0.06	4.0	0.07	42.0
B 28.75-1	*steinheimensis*	3.15	27.3	−2.5	0.11	3.0	0.11	41.0
B 28.75-2	*steinheimensis*	3.15	38.2	−1.8	0.10	2.2	0.07	40.1
B 29.2-3	*steinheimensis*	2.7	29.5	−2.2	0.09	4.0	0.09	42.0
B 29.2-4	*steinheimensis*	2.7	26.2	−1.6	0.11	1.3	0.08	39.2
B 29.6-3	*steinheimensis*	2.35	8.8	−1.4	0.10	0.9	0.08	38.8
B 29.6-4	*steinheimensis*	2.35	5.1	−2.1	0.11	3.9	0.09	41.9
B 30.0-3	*steinheimensis*	1.75	43.4	−2.3	0.09	3.1	0.08	41.1
B 30.0-4	*steinheimensis*	1.75	38.5	−2.7	0.12	2.6	0.09	40.6
B 31.8-1	*steinheimensis*	0.1	13.5	−1.1	0.12	1.3	0.08	39.3
B 31.8-2	*steinheimensis*	0.1	4.0	−0.7	0.10	2.7	0.09	40.6
Gf 2-1	*steinheimensis*	−3	2.7	-3.6	0.12	1.2	0.08	39.1
Gf 2-2	*steinheimensis*	−3	1.1	−4.9	0.11	−3.6	0.10	34.1
Ge 5-1	*steinheimensis*	−3.5	12.8	−6.0	0.17	1.4	0.11	39.4
Ge 5-4	*steinheimensis*	−3.5	6.3	−4.1	0.06	2.9	0.09	40.9
Ge 4-1	*kleini*	−4	4.4	−0.7	0.04	2.8	0.08	40.8
Ge 4-2	*kleini*	−4	2.3	−2.1	0.05	2.1	0.09	40.1
Ge 1-1	*kleini*	−4.58	8.4	−4.3	0.07	−2.2	0.07	35.6
Ge 1-2	*kleini*	−4.5	9.6	−1.4	0.07	−0.2	0.08	37.7

$n=89$) and $\delta^{13}C$ values range from −4.0 to +1.9‰ ($\delta^{13}C=-1.1\pm1.3$‰, $n=89$). Lowest $\delta^{18}O$ and $\delta^{13}C$ values occur in the basal *kleini* beds (Table 9, Fig. 4). Shells of *Gyraulus* spp. have similar $\delta^{18}O$ and $\delta^{13}C$ values compared to those of the ostracod *I. binocularis* (Fig. 4). $\delta^{18}O$ values of both, ostracods and freshwater gastropods, are high and scatter around a mean value of +2‰ throughout the whole succession of lake sediments, except for those from the basal *kleini* beds with lower $\delta^{18}O$ values (Fig. 4). The $\delta^{13}C$ values of the *Gyraulus* gastropods and ostracods also display the same trend over the complete succession of the 7 gastropod beds (Fig. 4), with $\delta^{13}C$ values increasing continuously from the *kleini* period up until the *trochiformis* period, the major lake level low-stand phase. After a decrease during the *trochiformis/oxystoma* period the $\delta^{13}C$ values increase again reaching the highest $\delta^{13}C$ values in the final *supremus* period and thus the end of sedimentation in the lake (Fig. 4). The $\delta^{13}C$ values seem to follow the known lake level fluctuations (Fig. 4).

The aragonitic shells of the land snail *Megalotrochlea sylvestrina* have $\delta^{18}O$ values ranging from −2.2 to −1.3‰ ($\delta^{18}O=-1.8\pm0.3$‰, $n=4$) and $\delta^{13}C$ values range from −6.1 to −3.3‰ ($\delta^{13}C=-4.6\pm1.2$‰, $n=4$) (Fig. 5).

4.3. C and O isotope compositions of fish teeth and otoliths

The abundant *T. micropygoptera* and rare *B. steinheimensis* have similar carbon and oxygen isotope compositions for their teeth and vary only within a narrow range. The $\delta^{18}O_{CO3}$ values range from −2.5 to −1.1‰ ($\delta^{18}O_{CO3}=-1.8\pm0.4$‰, $n=17$), $\delta^{18}O_{PO4}$ values from 23.0 to 25.7‰ ($\delta^{18}O_{PO4}=24.3\pm0.8$‰, $n=9$) while the $\delta^{13}C$ values range from −7.5 to −5.8‰ ($\delta^{13}C=-6.5\pm0.6$‰, $n=17$) (Table 3). The *T. micropygoptera* teeth from the fish layer in the *sulcatus* beds have the same isotopic compositions as those of the *trochiformis/oxystoma* beds, the mammal-bearing layer (Fig. 4). Otoliths of *T. micropygoptera*, all from the fish

Table 10
O and C isotopic compositions of ostracod carapaces

Sample	Ostracod species	Profile (m)	Number of valves	Weight µg	$\delta^{13}C$ [‰] VPDB	σ	$\delta^{18}O$ [‰] VPDB	σ	$\delta^{18}O$ [‰] VSMOW
K 19	*Ilyocypris binocularis*	22.4	1	30	1.4	0.06	3.8	0.11	34.8
K 14	*Ilyocypris binocularis*	21.5	2	29	0.8	0.05	1.9	0.13	32.8
K 14	*Ilyocypris binocularis*	21.5	2	43	0.8	0.07	1.1	0.14	32.1
K 12	*Ilyocypris binocularis*	21.2	1	39	0.4	0.06	2.8	0.15	33.8
K 12	*Ilyocypris binocularis*	21.2	1	33	1.1	0.08	3.3	0.15	34.4
K 12	*Ilyocypris binocularis*	21.2	1	27	0.5	0.08	2.1	0.12	33.1
K 8	*Ilyocypris binocularis*	20.4	1	28	0.1	0.07	2.0	0.14	32.9
K 8	*Ilyocypris binocularis*	20.4	1	32	0.0	0.09	2.4	0.17	33.4
K 5	*Ilyocypris binocularis*	20.2	1	25	0.1	0.08	0.4	0.12	31.3
K 5	*Ilyocypris binocularis*	20.2	1	26	0.3	0.06	2.3	0.12	33.3
K 1	*Ilyocypris binocularis*	19.6	1	27	0.1	0.07	0.4	0.13	31.3
K 1	*Ilyocypris binocularis*	19.6	1	28	0.9	0.06	1.2	0.15	32.2
Ph 20	*Ilyocypris binocularis*	19.6	2	29	−0.3	0.05	2.5	0.13	33.5
Ph 16	*Ilyocypris binocularis*	18.9	3	66	−0.9	0.11	1.2	0.13	32.1
Ph 16	*Ilyocypris binocularis*	18.9	3	67	−0.2	0.09	1.8	0.11	32.7
Ph 16	*Ilyocypris binocularis*	18.9	3	88	0.0	0.11	2.8	0.12	33.7
Ph 16	*Ilyocypris binocularis*	18.9	2	49	0.5	0.10	3.0	0.14	34.0
Ph 12	*Ilyocypris binocularis*	18.3	1	29	−0.1	0.09	3.5	0.16	34.5
Ph 12	*Ilyocypris binocularis*	18.3	1	21	−1.4	0.17	−0.6	0.13	30.3
Ph 10	*Ilyocypris binocularis*	18	1	36	0.5	0.07	3.3	0.14	34.3
Ph 10	*Ilyocypris binocularis*	18	1	22	−1.3	0.11	−0.2	0.13	30.7
Ph 8	*Ilyocypris binocularis*	17.7	1	25	−1.6	0.10	1.8	0.18	32.8
Ph 8	*Ilyocypris binocularis*	17.7	1	26	−1.0	0.15	1.5	0.17	32.5
Ph 6	*Ilyocypris binocularis*	17.4	1	20	−1.9	0.14	0.1	0.21	31.0
Ph 6	*Ilyocypris binocularis*	17.4	1	19	−1.2	0.10	−0.3	0.10	30.6
Ph 4	*Ilyocypris binocularis*	17.1	1	25	−0.6	0.08	2.9	0.16	33.9
Ph 4	*Ilyocypris binocularis*	17.1	1	27	−0.2	0.11	3.0	0.12	34.0
PH 2	*Ilyocypris binocularis*	16.6	3	58	−0.7	0.07	2.1	0.07	33.1
PH 2	*Ilyocypris binocularis*	16.6	4	89	−0.5	0.11	2.5	0.10	33.5
PH 2	*Ilyocypris binocularis*	16.6	3	64	−0.5	0.11	1.4	0.20	32.4
S 37	*Ilyocypris binocularis*	16.5	1	34	−0.7	0.04	2.3	0.13	33.3
S 37	*Ilyocypris binocularis*	16.5	1	29	−0.6	0.11	2.6	0.16	33.6
S 35	*Ilyocypris binocularis*	16.3	2	34	−0.3	0.06	1.8	0.17	32.8
S 33	*Ilyocypris binocularis*	15.6	2	31	−0.1	0.10	0.3	0.16	31.2
S 33	*Ilyocypris binocularis*	15.6	2	36	0.8	0.07	1.5	0.09	32.5
S 33	*Ilyocypris binocularis*	15.6	2	35	0.2	0.23	1.1	0.13	32.1
S 33	*Pseudocandona steinheimense*	15.6	2	30	1.9	0.12	2.8	0.18	33.8
S 33	*Pseudocandona steinheimense*	15.6	3	45	0.5	0.19	3.3	0.17	34.3
S 31	*Ilyocypris binocularis*	15.2	1	19	0.1	0.13	3.0	0.19	34.0
S 31	*Ilyocypris binocularis*	15.2	2	32	0.1	0.07	2.4	0.15	33.4
S 27	*Ilyocypris binocularis*	14.7	2	37	0.3	0.14	0.3	0.17	31.2
S 21	*Ilyocypris binocularis*	13.7	1	28	−1.6	0.10	2.7	0.26	33.7
S 21	*Ilyocypris binocularis*	13.7	1	22	−0.5	0.11	2.6	0.17	33.5
S 17	*Ilyocypris binocularis*	13.3	1	25	−0.7	0.13	3.4	0.20	34.4
S 17	*Ilyocypris binocularis*	13.3	2	35	−0.4	0.07	3.6	0.13	34.6
S 15	*Ilyocypris binocularis*	13.2	2	31	−1.6	0.08	1.1	0.18	32.0
S 15	*Ilyocypris binocularis*	13.2	2	27	−1.3	0.10	1.0	0.17	31.9
S 13	*Ilyocypris binocularis*	13	2	33	−0.6	0.10	2.8	0.15	33.8
S 13	*Ilyocypris binocularis*	13	2	33	−0.9	0.10	2.0	0.18	33.0
S 10	*Ilyocypris binocularis*	12.8	3	42.5	−0.5	0.09	1.1	0.15	32.1
S 10	*Ilyocypris binocularis*	12.8	4	55.4	−1.1	0.11	1.1	0.22	32.0
S 10	*Ilyocypris binocularis*	12.8	3	41.7	−0.2	0.08	1.7	0.13	32.6
S 8	*Ilyocypris binocularis*	12.6	2	31	−1.4	0.14	0.8	0.18	31.8
SF 9	*Ilyocypris binocularis*	10.8	2	33	0.2	0.09	3.1	0.12	34.1
S 1	*Ilyocypris binocularis*	11.2	2	24	−0.9	0.11	0.5	0.12	31.4
SF 11	*Ilyocypris binocularis*	10.4	2	25	−0.6	0.11	0.5	0.15	31.4

Table 10 (*continued*)

Sample	Ostracod species	Profile (m)	Number of valves	Weight µg	$\delta^{13}C$ [‰] VPDB	σ	$\delta^{18}O$ [‰] VPDB	σ	$\delta^{18}O$ [‰] VSMOW
SF 13	*Ilyocypris binocularis*	9.6	2	27	−1.1	0.17	−0.1	0.17	30.8
SF 13	*Ilyocypris binocularis*	9.6	2	32	−1.2	0.15	1.5	0.17	32.5
SF 16	*Ilyocypris binocularis*	8.9	2	23	−0.3	0.15	1.1	0.18	32.0
SF 18	*Ilyocypris binocularis*	7.8	2	38	−0.2	0.09	4.0	0.14	35.0
SF 18	*Ilyocypris binocularis*	7.8	2	30	−1.0	0.13	2.3	0.17	33.3
B 25.1–25.2	*Ilyocypris binocularis*	6.9	2	30	−1.0	0.12	0.4	0.16	31.3
B 25.1–25.2	*Ilyocypris binocularis*	6.9	2	34	−1.6	0.08	0.7	0.17	31.6
B 26.9–27.1	*Ilyocypris binocularis*	5	4	30	−1.0	0.09	0.9	0.12	31.9
B 28.1	*Ilyocypris binocularis*	3.9	2	19	−2.2	0.16	1.9	0.21	32.9
B 28.1	*Ilyocypris* sp.	3.9	3	19	−1.4	0.11	0.6	0.07	31.5
B 28.75–29	*Ilyocypris* sp.	3.2	3	31	−1.6	0.10	3.4	0.11	34.4
B 29.2–29.4	*Ilyocypris binocularis*	2.7	3	23	−0.9	0.09	1.2	0.16	32.2
B 29.2–29.4	*Ilyocypris* sp.	2.7	3	30	−1.4	0.09	3.2	0.12	34.2
B 29.6–29.7	*Ilyocypris binocularis*	2.4	3	32	−0.9	0.11	1.4	0.08	32.3
B 29.6–29.7	*Ilyocypris* sp.	2.4	3	25	−2.1	0.10	3.5	0.13	34.5
B 29.6–29.7	*Ilyocypris* sp.	2.4	3	24	−2.0	0.04	3.3	0.26	34.3
B 30.0–30.5	*Ilyocypris binocularis*	1.8	3	31	−1.8	0.08	0.8	0.09	31.7
B 30.0–30.5	*Ilyocypris* sp.	1.8	2	23	−1.5	0.11	2.5	0.16	33.5
B 31.8–32	*Ilyocypris binocularis*	0.1	7	29	−0.3	0.09	0.5	0.12	31.4
Gf 2	*Ilyocypris* sp. (*I. aff. gibba*)	−3	5	34	1.4	0.10	1.9	0.14	32.9
Ge 5	*Ilyocypris* sp. (*I. aff. gibba*)	−3.5	4	25	−3.6	0.09	−1.9	0.13	28.9
Ge 2	*Ilyocypris* sp. (*I. aff. gibba*)	−3.8	3	31	−3.1	0.09	−0.8	0.10	30.1
Ge 1	*Ilyocypris* sp. (*I. aff. gibba*)	−4.5	3	30	−5.1	0.08	−2.1	0.20	28.7
Gb 6	*Ilyocypris binocularis*	−4.7	2	35	−4.0	0.07	−2.3	0.15	28.5

Table 11
Sr isotopic composition of large and small mammal teeth

Sample	Material	Animal	Species	Locality	$^{87}Sr/^{86}Sr$	2σ
FZ CE ST 8	Enamel	Deer	*Micromeryx flourensianus*	Steinheim basin	0.707530	7
FZ EQ ST 2	Enamel	Horse	*Anchitherium aurelianense*	Steinheim basin	0.708142	13
FZ EQ ST 4	Enamel	Horse	*Anchitherium aurelianense*	Steinheim basin	0.707027	7
FZ EQ ST 5	Enamel	Horse	*Anchitherium aurelianense*	Steinheim basin	0.707722	9
FZ EQ ST 7	Enamel	Horse	*Anchitherium aurelianense*	Steinheim basin	0.707970	9
FZ MA ST 1	Enamel	Elephant	*Gomphotherium steinheimense*	Steinheim basin	0.708530	9
FZ MA ST 2	Enamel	Elephant	*Gomphotherium steinheimense*	Steinheim basin	0.707537	11
FZ MA ST 3	Enamel	Elephant	*Gomphotherium steinheimense*	Steinheim basin	0.708567	9
FZ PA ST 1	Enamel	Antelope	*Palaeomeryx eminens*	Steinheim basin	0.708643	10
FZ RH ST 5	Enamel	Rhinoceros	*Brachypotherium brachypus*	Steinheim basin	0.708015	9
FZ RH ST 9	Enamel	Rhinoceros	*Lartetotherium sansaniense*	Steinheim basin	0.707954	8
FZ RH ST 2	Enamel	Rhinoceros	*Dicerorhinus steinheimensis*	Steinheim basin	0.708250	10
FZ RO ST 6	Tooth	Rodent	rodent indet.	Steinheim basin	0.707535	8
FZ GA ST 3	Tooth	Hairy hedgehog	*Galerix socialis*	Steinheim basin	0.707815	10
FZ LA ST 3	Tooth	Pika	*Prolagus oeningensis*	Steinheim basin	0.707509	83
FZ LA ST 5	Tooth	Pika	*Prolagus oeningensis*	Steinheim basin	0.708043	8
FZ LA ST 6	Tooth	Pika	*Prolagus oeningensis*	Steinheim basin	0.707455	7
FZ LA ST 7	Tooth	Pika	*Prolagus oeningensis*	Steinheim basin	0.707856	9
FZ EQ EN 2	Enamel	Horse	*Anchitherium aurelianense*	Engelswiese	0.707871	10
FZ EQ HW 3	Enamel	Horse	*Hippotherium primigenium*	Höwenegg	0.706241	7
FZ EQ NÖ 1	Enamel	Horse	*Anchitherium aurelianense*	Nördlinger Ries	0.707027	7
FZ EQ NÖ 3	Enamel	Horse	*Anchitherium aurelianense*	Nördlinger Ries	0.707857	7
FZ EQ SA 1	Enamel	Horse	*Anchitherium aurelianense*	Sandelzhausen	0.710319	9
FZ MA SA 4	Enamel	Elephant	*Gomphotherium angustidens*	Sandelzhausen	0.710427	10
FZ MA HE 2	Enamel	Elephant	*Gomphotheriidae*	Helsighausen	0.708476	10
FZ MA HÜ 1	Enamel	Elephant	*Gomphotherium angustidens*	Hüllistein	0.708273	8
FZ RH LA 4	Enamel	Rhinoceros	*Brachypotherium brachypus*	Ulm Langenau	0.708674	8

Table 12
Sr isotopic composition of aquatic fossils from the Steinheim basin

Sample	Material	Animal	Species	Locality	$^{87}Sr/^{86}Sr$	2σ
FK SCH ST 14	Bone	Turtle	*Clemmydopsis turnauensis*	Steinheim basin	0.707563	8
FK SCH ST 9	Bone	Turtle	*Chelydropsis murchisoni*	Steinheim basin	0.707503	9
FZ SL ST 6	Tooth	Fish	*Tinca micropygoptera*	Steinheim basin	0.707514	7
OT SL ST 14	Aragonite otolith	Fish	*Tinca micropygoptera*	Steinheim basin	0.707437	7
SCH 4	Aragonite shell	Gastropod	*Megatrochlea sylvestrina*	Steinheim basin	0.707413	10
K 19-3	Aragonite shell	Gastropod	*Gyraulus supremus*	Steinheim basin	0.707464	8
K 5-1	Aragonite shell	Gastropod	*Gyraulus oxystoma*	Steinheim basin	0.707338	7
OXY 5	Aragonite shell	Gastropod	*Gyraulus oxystoma*	Steinheim basin	0.707461	11
Ph 16-3	Aragonite shell	Gastropod	*Gyraulus oxystoma*	Steinheim basin	0.707440	8
ST S 35-3	Aragonite shell	Gastropod	*Gyraulus trochiformis*	Steinheim basin	0.707418	9
S 31-1	Aragonite shell	Gastropod	*Gyraulus trochiformis*	Steinheim basin	0.707410	9
ST S 21-3	Aragonite shell	Gastropod	*Gyraulus trochiformis*	Steinheim basin	0.707483	9
ST SF 9-3	Aragonite shell	Gastropod	*Gyraulus sulcatus*	Steinheim basin	0.707467	7
ST B 28.75-2	Aragonite shell	Gastropod	*Gyraulus steinheimensis*	Steinheim basin	0.707463	9
ST Ge 1-2	Aragonite shell	Gastropod	*Gyraulus kleini*	Steinheim basin	0.707375	8

layer in the *sulcatus* beds, have $\delta^{18}O$ values that range from +0.5 to +1.5‰ ($\delta^{18}O = +1.0 \pm 0.3$‰, $n=11$) and $\delta^{13}C$ values that range from −9.5 to −13‰ ($\delta^{13}C = -11.8 \pm 1$‰, $n=11$) (Table 7). In contrast to the phosphatic fish teeth, the aragonitic otoliths of *T. micropygoptera* have 3‰ higher $\delta^{18}O$ and 5‰ lower $\delta^{13}C$ values (Fig. 5). One otolith of the *kleini* beds has a 6‰ lower $\delta^{18}O$ value of −5.2‰ than the other otoliths but a similar $\delta^{13}C$ value of −9.9‰.

4.4. C and O isotope compositions of turtle bones

Carapace bones of two freshwater turtles, the carnivorous *C. murchisoni* and the herbivorous *C. turnauensis* have similar oxygen and carbon isotopic compositions (Table 4). $\delta^{18}O_{CO3}$ values range from −0.6 to −2.4‰ ($\delta^{18}O_{CO3} = -1.2 \pm 0.7$‰, $n=15$), $\delta^{18}O_{PO4}$ values from 23.4 to 24.6‰ ($\delta^{18}O_{PO4} = 24.1 \pm 0.4$‰, $n=6$) and the $\delta^{13}C$ values range from −8.4 to −8.0‰ ($\delta^{13}C = -8.2 \pm 0.2$‰, $n=15$). The bones of the land turtle *Testudo* sp. have $\delta^{18}O_{CO3}$ values ranging from −0.6 to −1.5‰ ($\delta^{18}O_{CO3} = -0.6 \pm 0.5$‰, $n=6$) and $\delta^{13}C$ values that range from −8.6 to −7.7‰ ($\delta^{13}C = -8.2 \pm 0.3$‰, $n=6$), similar to those of the aquatic turtles (Table 4).

4.5. C and O isotope compositions of large mammal teeth

Enamel samples of all large mammal taxa (equids, proboscideans, suids, cervids, rhinocerotids, palaeomerycids) have $\delta^{18}O_{CO3}$ values that range from −8.6 to −1.8‰ ($\delta^{18}O_{CO3} = -5.8 \pm 1.9$‰, $n=40$) (Fig. 5), $\delta^{18}O_{PO4}$ values from 15.9 to 24.0‰ ($\delta^{18}O_{PO4} = 18.4 \pm 2.0$‰, $n=33$) (Table 1). Most enamel samples have $\delta^{18}O_{PO4}$ values of between 15.9 and 20.4‰, only those of two teeth from *Palaeomeryx eminens*, an extinct giraffe-like mammal, have very high $\delta^{18}O_{PO4}$ values of 23.6 and 24.0‰. Based on their dental morphology palaeomerycids are browsers thus these high $\delta^{18}O_{PO4}$ values are probably due to uptake of ^{18}O-enriched leaf water. Excluding these two evaporative influenced *Palaeomeryx* samples all other large mammal enamel samples have a mean $\delta^{18}O_{PO4}$ value of 18.1 ± 1.5‰ ($n=31$).

$\delta^{13}C$ values for all enamel samples range from −13.7 to −8.9‰ ($\delta^{13}C = -11.1 \pm 1.1$‰, $n=40$) (Fig. 5). Only the enamel samples of the large rhinoceros *Brachypotherium brachypus* have a 2‰ lower mean $\delta^{13}C$ value of −13.1 ± 0.6‰ ($n=5$).

Table 13
Sr isotopic composition of modern ground- and surface water from the Steinheim basin

Sample	Water type	Aquifer geology	Water souce	Locality	$^{87}Sr/^{86}Sr$	2σ
H_2O ST 4	Groundwater	Up. Jurassic limestone	Well Sontheim	Steinheim basin	0.707734	9
H_2O ST 5	Surface water	Mid. Jurassic claystone	Lettenhülbe, pond on central hill	Steinheim basin	0.711219	9
H_2O ST 8	Groundwater	Mid. Jurassic claystone	Well Eschental	Steinheim basin	0.707352	10
H_2O ST 9	Groundwater	Up. Jurassic limestone	Well Hirschtal	Steinheim basin	0.707870	15
H_2O ST 10	Groundwater	Up. Jurassic limestone	Well Rohrbrunnen	Steinheim basin	0.707547	9

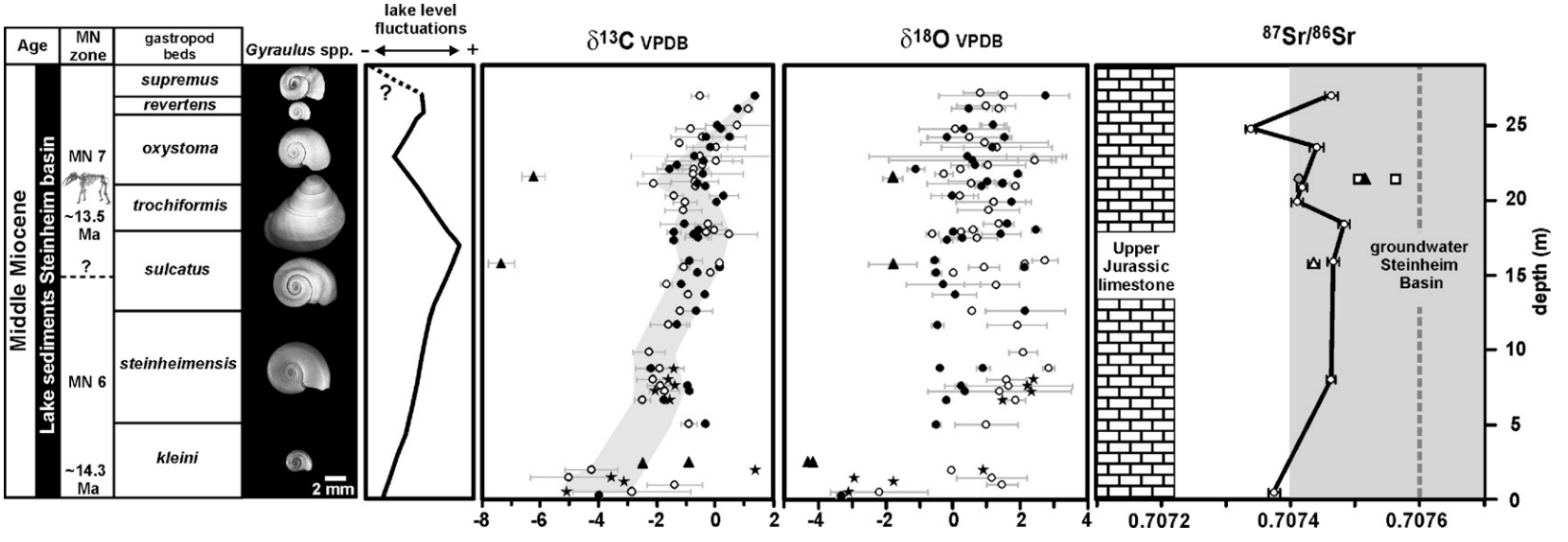

Fig. 4. Mean C, O, and Sr isotope values and standard deviations of skeletal tissues from sympatric freshwater organisms from sediment samples covering the complete lake sediment profile with all 7 *Gyraulus* gastropod beds. Gastropod shells: ? (*Gyraulus* spp.), benthic ostracod valves: ● (*I. binocularis*) and ★ (*Ilyocypris* sp.), ▲ fish teeth and △ otolith of *T. micropygoptera*, ○ aquatic turtle bone. For illustration a photograph of one shell of each *Gyraulus* species is given. Stratigraphy is as in Fig. 2b. The lake level fluctuations are based on sedimentologic data after Mensink (1984).

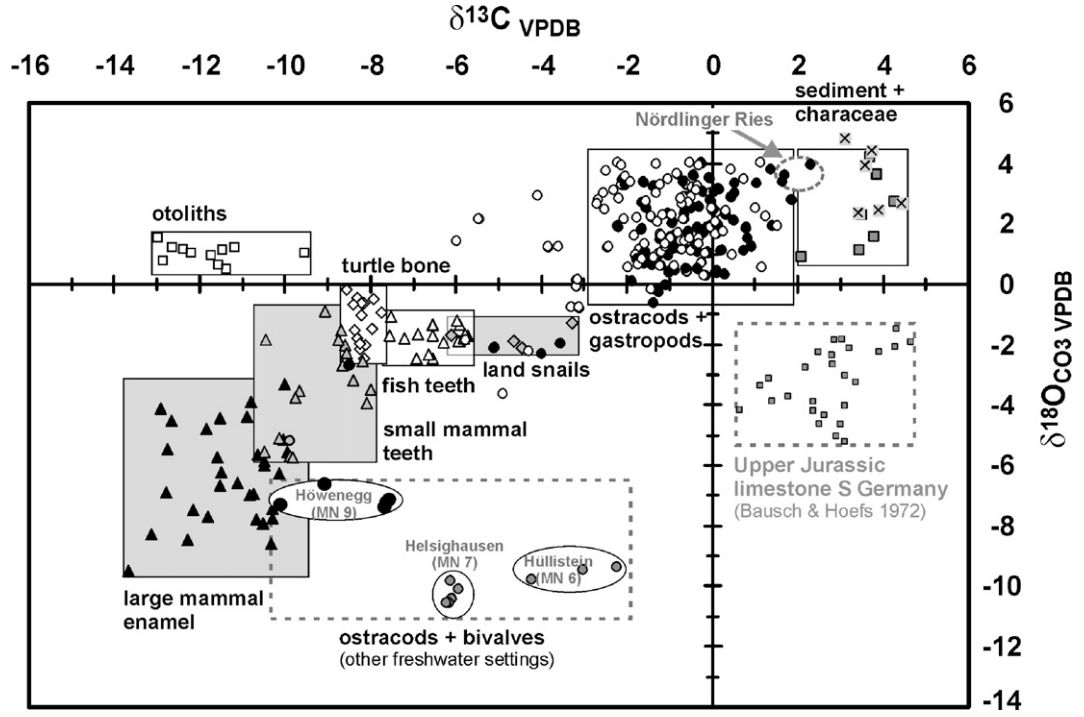

Fig. 5. Plot of the $\delta^{18}O_{CO3}$ and $\delta^{13}C$ values of all terrestrial (grey shaded boxes) and aquatic vertebrate and invertebrate skeletal remains (white boxes) of the Steinheim basin. For comparison, isotopic compositions of biogenic carbonates from other penecontemporaneous Miocene freshwater settings (Table 8) and from the Upper Jurassic limestone of the Swabian Alb after Bausch and Hoefs (1972) are also plotted.

4.6. C and O isotope compositions of small mammal teeth

Because of the scarcity of small mammal remains, only 14 teeth and 3 jaw bone samples belonging to hairy hedgehogs (*Galerix socialis*), pikas (*P. oeningensis*) and rodents could be sacrificed for isotopic analyses (Table 2). To get sufficient material for isotope analysis the whole teeth had to be used. The $\delta^{18}O_{CO3}$ values of those small mammal teeth range from −5.7 to −0.9‰ ($\delta^{18}O_{CO3}=-3.5\pm1.7$‰, $n=13$), $\delta^{18}O_{PO4}$ values from 15.9 to 24.9‰ ($\delta^{18}O_{PO4}=20.4\pm2.9$‰, $n=14$) while the $\delta^{13}C$ values range from −10.5 to −8.0‰ ($\delta^{13}C=-9.2\pm0.8$‰, $n=13$) (Fig. 5). In contrast to the enamel of large mammal teeth ($\delta^{18}O_{PO4}=18.4\pm2.0$‰, $n=14$), small mammal teeth have on average 2‰ higher $\delta^{18}O_{PO4}$ values and a larger standard deviation. The teeth from the abundant pika *P. oeningensis* ($\delta^{18}O_{PO4}=19.5\pm3.0$‰, $n=7$) have a 2‰ lower $\delta^{18}O_{PO4}$ value than those of rodent teeth ($\delta^{18}O_{PO4}=21.6\pm3.3$‰, $n=5$).

4.7. Sr isotope compositions of modern water samples

Results of the Sr isotopic composition ($^{87}Sr/^{86}Sr$) for modern groundwater and surface water samples from the Steinheim basin are given in Table 13. $^{87}Sr/^{86}Sr$ ratios of groundwater samples from 3 wells in the Steinheim basin range from 0.707352 to 0.707870 ($^{87}Sr/^{86}Sr=0.70763\pm0.00023$, $n=4$). Though all these samples are presumably from an Upper Jurassic limestone aquifer the $^{87}Sr/^{86}Sr$ ratios are well above the Sr isotopic composition to be expected for the dissolution of Upper Jurassic marine limestone ($^{87}Sr/^{86}Sr=0.70697$ to 0.70722, McArthur et al., 2001, Fig. 4). This indicates input of dissolved more radiogenic Sr from another source e.g. clayey rock members of the Upper Jurassic strata like the marls of the underlying "Zementmergel" (Malm ζ 2) or intercalated marly layers in the Upper Jurassic (Malm ζ 3) limestone forming the Swabian Alp plateau in the vicinity of the Steinheim Basin. Furthermore, the Middle Jurassic silt- and claystones, which are part of the impact breccia and form the central hill, can supply Sr with high $^{87}Sr/^{86}Sr$ ratios as indicated by a surface water sample ($^{87}Sr/^{86}Sr=0.711219$) from a little pond from the top of the central hill based on Middle Jurassic Opalinus Clay.

4.8. Sr isotope compositions of aquatic fossil remains

$^{87}Sr/^{86}Sr$ ratios of the gastropod *Gyraulus* from all 7 gastropod beds cover a narrow range from 0.707338 to

0.707483 ($^{87}Sr/^{86}Sr = 0.70743 \pm 0.00005$, $n = 10$; Table 12). The Sr isotopic composition of the *Gyraulus* shells appears to be positively correlated with the lake level fluctuations reconstructed from sedimentological data (Fig. 4). The Sr isotopic compositions of the gastropod shells increase from a $^{87}Sr/^{86}Sr$ ratio of 0.707375 in the basal *kleini* beds towards the maximum value of 0.707483 in the lower *trochiformis* beds. After a two-step decrease the $^{87}Sr/^{86}Sr$ ratio reaches the minimum value of 0.707338 in the middle *oxystoma* beds. Afterwards the $^{87}Sr/^{86}Sr$ increases again to a value of 0.70746 in the *supremus* beds (Fig. 4).

The $^{87}Sr/^{86}Sr$ ratio of the land snail *Megalotrochea sylvestrina* ($^{87}Sr/^{86}Sr = 0.707413$) as well as one otolith of *T. micropygoptera* ($^{87}Sr/^{86}Sr = 0.707437$) from the fish layer falls within the range of the *Gyraulus* spp. gastropods (Fig. 4). The phosphatic fish tooth of *T. micropygoptera* ($^{87}Sr/^{86}Sr = 0.707514$) and the carapace bone of the aquatic turtles *C. turnauensis* ($^{87}Sr/^{86}Sr = 0.707563$) and *Chelydropsis murchinsoni* ($^{87}Sr/^{86}Sr = 0.707503$), however, have slightly higher $^{87}Sr/^{86}Sr$ values than all *Gyraulus* gastropod shells (Fig. 4).

4.9. Sr isotope compositions of teeth from large and small mammals

Sr isotopic compositions of the large and small mammal teeth are given in Table 11. The enamel $^{87}Sr/^{86}Sr$ ratios for large mammal teeth from the Steinheim basin range from 0.707027 to 0.708643 ($^{87}Sr/^{86}Sr = 0.7080 \pm 0.0005$, $n = 12$) while $^{87}Sr/^{86}Sr$ ratios of small mammal teeth range from 0.707509 to 0.708043 ($^{87}Sr/^{86}Sr = 0.7077 \pm 0.0002$, $n = 6$) having a narrower range similar to that of modern groundwater samples from the Steinheim basin (Table 13).

For comparison, the Sr isotopic composition of enamel samples from large mammal teeth from other Miocene localities in the Molasse basin and from SW Germany and Switzerland have also been analysed (Table 11). These enamel samples have $^{87}Sr/^{86}Sr$ ratios ranging from 0.706241 to 0.710427 ($n = 9$) covering and exceeding the range of $^{87}Sr/^{86}Sr$ ratios from the mammal teeth of the Steinheim basin.

5. Discussion

5.1. Diagenesis of the biogenic carbonates and phosphates

In order to allow for an integrative palaeoenvironmental and -ecologic reconstruction on the basis of the isotopic composition of fossils it is essential that the original chemical composition of the skeletal remains is preserved. Because the carbonaceous lake sediments of the Steinheim basin themselves have been preserved as original aragonite (Wolff and Füchtbauer, 1976) a severe diagenetic alteration of the sediments and the fossil remains therein is considered unlikely. This is supported by the *Gyraulus* gastropod shells that have preserved their original aragonite and even parts of their amino acids (Degens and Steven, 1965). It can therefore be assumed that the aragonitic gastropod shells, as well as the more stable calcitic ostracod valves, have also preserved their pristine C, O, and Sr isotopic compositions, as isotopic exchange at low temperatures is generally facilitated through chemical/mineralogical reactions. This does not exclude that fossils may contain early diagenetic aragonite cements (Wolff and Füchtbauer, 1976). However, the sampling strategy avoided specimens that contained visible contamination and/or pre-treated the samples to remove diagenetic carbonate (see Section 3).

The biogenic phosphate of enamel, tooth, and bone samples from the Steinheim basin plot relatively close and parallel to the expected $\delta^{18}O_{CO3}$–$\delta^{18}O_{PO4}$ isotopic equilibrium line for modern mammal bones (Fig. 6). However, for the enamel of the large mammal teeth the mean difference of the $\delta^{18}O_{CO3}$–$\delta^{18}O_{PO4}$ values is 6.6± 1.5‰ ($n = 50$), which is about 2‰ lower than the expected offset of 8.5 to 9.1‰ for modern mammal bones and teeth (Bryant et al., 1996; Iacumin et al., 1996). For some samples the difference between $\delta^{18}O_{CO3}$ and $\delta^{18}O_{PO4}$ values deviates several permille from the expected equilibrium value. Isotopic compositions are likely biased to some degree for the whole teeth of the small mammals and fish, which represent a mixture of enamel, which is more robust to diagenetic alteration, and dentine, which is less robust to such alteration. The same will apply to bone samples. These samples often have a higher carbonate content >6 wt.% than pure enamel samples (Tables 1–4) and some diagenetic change at least of the carbonate in the phosphate of the dentine is likely. Thus when using small mammal or fish teeth it is in general preferable to analyse only enamel rather than complete teeth even if this requires a mixing of enamel from a number of sympatric teeth. Tooth enamel of the large mammals has, however, retained low average carbonate contents of 4.8±1.1 wt.% ($n = 40$) that is only slightly higher than that of modern enamel (e.g., Schumacher and Schmidt, 1983: 2.3 to 3.5 wt.%). Furthermore, the original enamel carbon isotopic composition seems to be preserved because enamel $\delta^{13}C$ values of the large mammal teeth are

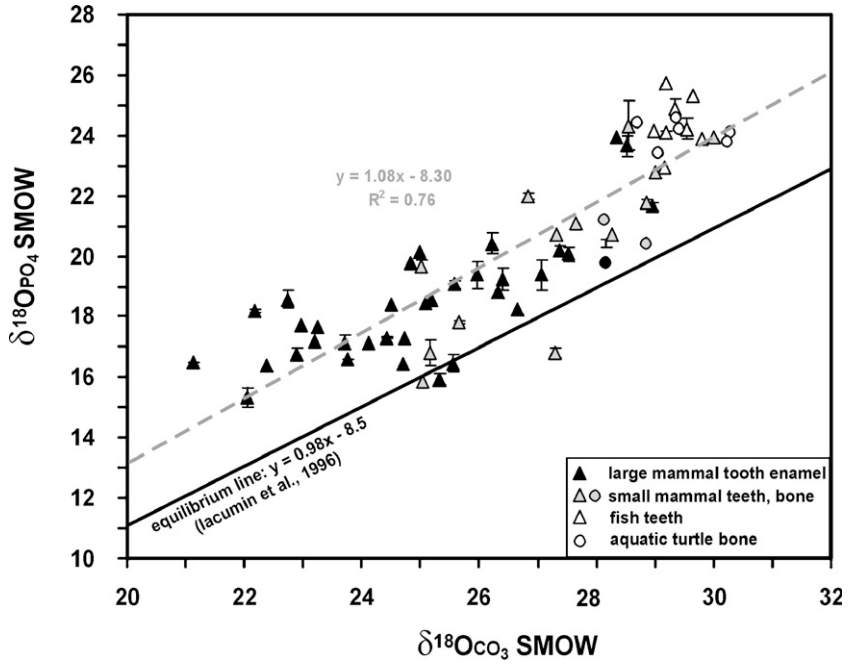

Fig. 6. $\delta^{18}O_{CO3}$ vs. $\delta^{18}O_{PO4}$ values of all vertebrate skeletal remains from the Steinheim basin. The regression line parallels the equilibrium line of Iacumin et al. (1996).

much lower ($\delta^{13}C = -11.1 \pm 1.1‰$, $n=40$) than those for the embedding sediments ($\delta^{13}C$ about +3.5‰), and the teeth have values typical for a C_3 plant diet. This suggests that the enamel samples may well have preserved their original isotopic compositions. As the phosphate oxygen is generally considered to be more resistant to exchange with water under inorganic conditions than that of carbonate in the phosphate (e.g., Zazzo et al., 2004), the skeletal apatite $\delta^{18}O_{PO4}$ values are probably preserved. If, however, diagenetic alteration was important, then the $\delta^{18}O$ values are potentially biased towards more positive $\delta^{18}O$ values as the lake water was ^{18}O-enriched (Bajor, 1965; this study). The enamel samples of the large mammal teeth, though fossilized in the same ^{18}O-rich lake water, still have 6±2‰ lower $\delta^{18}O_{PO4}$ values compared to sympatric aquatic turtle bones (Fig. 6), reflecting significant differences in drinking water $\delta^{18}O_{H2O}$ values between these.

Hence, while diagenetic alteration cannot readily be excluded, the fact that the samples plot in distinctive groups of carbon and oxygen isotopic compositions (Fig. 5) and this in good agreement with their different habitats, diets, and drinking water consumption, would suggest that the isotopic compositions have not been substantially modified. A severe diagenetic alteration would have attenuated or erased such primary isotopic differences. Therefore, a relatively reliable geochemical reconstruction of palaeoenvironmental and palaeoclimatic conditions based on isotopic compositions of the fossil remains is possible for the setting of the Steinheim basin.

5.2. $\delta^{18}O$ values of the biogenic carbonates — an archive for the lake water evaporation

The high $\delta^{18}O$ values of the skeletal tissues of all freshwater organisms from the Steinheim basin are generally similar to marine but atypical for freshwater biogenic carbonates (Fig. 5, Table 8). This may be explained by strong ^{18}O enrichment of the lake water due to evaporation of water from the long-term lake in the closed Steinheim basin (Bajor, 1965). These high values are also well in accordance with the reconstructed $\delta^{18}O_{H2O}$ value of around +2‰ (see Section 5.3. below) for the lake water of the Steinheim basin during the *trochiformis*/*oxystoma* period (Fig. 7). Evaporative ^{18}O enrichment is known from the lake in the neighbouring Nördlinger Ries, where $\delta^{18}O$ values of up to +6.5‰ have been recorded in the carbonaceous lake sediments (Rothe and Hoefs, 1977). On the basis of travertine $\delta^{18}O$ values Pache et al. (2001) also estimated a $\delta^{18}O_{H2O}$ value of about +2‰ for the Nördlinger Ries lake water. Freshwater $\delta^{18}O_{H2O}$ values of this magnitude are also

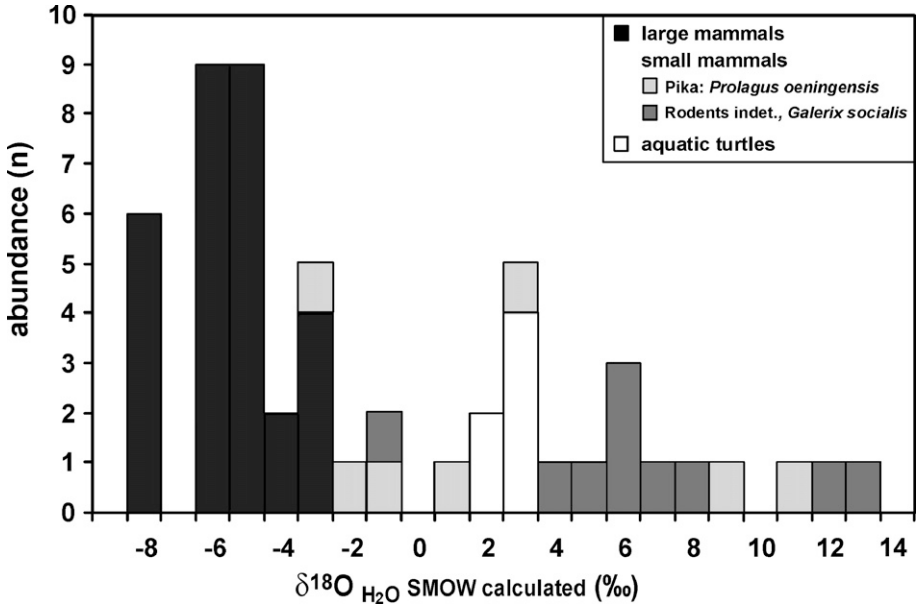

Fig. 7. Histogram of $\delta^{18}O_{H2O}$ values calculated from $\delta^{18}O_{PO4}$ values of small and large mammal teeth and aquatic turtle carapace bone using existing species-specific calibrations for extant vertebrates (Table 14).

typical for the epilimnion of deep meromictic lakes in warm, sub-tropical climate zones such as Lake Malawi ($\delta^{18}O_{H2O}$=+1.7 to +2.1‰) or Lake Tanganyika ($\delta^{18}O_{H2O}$=+3.4 to +4.2‰) in Central and East Africa (Gat, 1995 and references therein). Under cooler and more humid conditions such evaporation-influenced values are less common and the mean hydrogen and oxygen isotope composition of lake water lie closer to mean values for meteoric water (Gonfiantini, 1986; Gat, 1995). The lake water of the Steinheim basin probably became enriched in ^{18}O soon after the *kleini* period and the $\delta^{18}O_{H2O}$ value of around +2‰ was probably retained throughout nearly all of the existence of the lake (Fig. 4). The variations in $\delta^{18}O$ values of the gastropods and ostracods, which scatter without systematic variations around values of +2.0±1.3‰ and +1.7±1.2‰, respectively, (Fig. 4), thus probably reflect short term oscillations in water temperature and/or inflow-evaporation balance throughout the post-*kleini* period.

5.3. Calculation of the $\delta^{18}O_{H2O}$ value and lake water temperatures

To calculate water temperatures (T_{H2O}) for freshwater settings on the basis of oxygen isotope compositions of skeletal tissues from aquatic organisms it is necessary to know the $\delta^{18}O_{H2O}$ value. The oxygen isotope composition of the lake water from the Steinheim basin was calculated using the $\delta^{18}O_{PO4}$–$\delta^{18}O_{H2O}$ Eq. (1) for aquatic turtle bone from Barrick et al. (1999).

$$\delta^{18}O_{H2O} = 1.01(\delta^{18}O_{PO4}) - 22.3 \quad (1)$$

From the mean bone $\delta^{18}O_{PO4}$ value of 24.1±0.4‰ for the two aquatic turtles *C. murchisoni* and *C. turnauensis* a $\delta^{18}O_{H2O}$ value of +2.0±0.4‰ is calculated.

The approach used to calculate ambient water temperatures during their respective growing seasons from skeletal $\delta^{18}O$ values of ostracod valves, gastropod shells, fish otoliths and teeth is based upon that described by Grimes et al. (2003). This approach is valid if the aquatic turtles lived in the same water with all the other freshwater organisms, which is only strictly the case for the upper *trochiformis*/lower *oxystoma* beds in which the vertebrate remains are found (Fig. 2). Because ostracod and gastropod $\delta^{18}O$ values scatter around a similar mean value throughout the whole lake sediment section, except for the basal *kleini* beds (Fig. 4), the lake water $\delta^{18}O_{H2O}$ value of +2.0‰ is assumed to be similar for the whole post-*kleini* period and water temperatures have been calculated only for this time interval.

The equations used for the T_{H2O} calculation for the different proxies are given in Table 14. Calculated mean T_{H2O} range from 17 to 22 °C (Fig. 8). The water temperature appears to have been relatively homogeneous as skeletal remains from pelagic (fish

Table 14
Equations for the calculation of $\delta^{18}O_{H2O}$, T_{H2O}, and MAT

Taxon	Sekletal material	Equation	Reference
Rhinocerotids	Enamel apatite	$\delta^{18}O_{H2O(VSMOW)}=(\delta^{18}O_{PO4(VSMOW)}-25.09)/1.31$	Tütken, unpublished data
Equids	Enamel apatite	$\delta^{18}O_{H2O(VSMOW)}=(\delta^{18}O_{PO4(VSMOW)}-22.6)/0.77$	Modified after Huertas et al. (1995)
Cervids	Enamel apatite	$\delta^{18}O_{H2O(VSMOW)}=(\delta^{18}O_{PO4(VSMOW)}-25.53)/1.13$	D'Angela and Longinelli (1990)
Proboscids	Enamel apatite	$\delta^{18}O_{H2O(VSMOW)}=(\delta^{18}O_{PO4(VSMOW)}-23.3)/0.94$	Ayliffe et al. (1992)
Suids	Enamel apatite	$\delta^{18}O_{H2O(VSMOW)}=(\delta^{18}O_{PO4(VSMOW)}-22.61)/0.85$	Longinelli (1984)
Small mammals	Tooth apatite	$\delta^{18}O_{H2O(VSMOW)}=((\delta^{18}O_{PO4(VSMOW)}-17.42)-0.24)/0.59$	From Grimes et al. (2003)
Aquatic turtles	Bone apatite	$\delta^{18}O_{H2O(VSMOW)}=1.01\ \delta^{18}O_{PO4(VSMOW)}-22.3$	Barrick et al. (1999)
Fish teeth	Tooth apatite	$T_{H2O}(°C)=113.4-4.38\ (\delta^{18}O_{PO4(VSMOW)}-\delta^{18}O_{H2O(VSMOW)})$	Longinelli and Nuti (1973)
Gastropods (*Gyraulus* spp.)	Aragonite shell	$T_{H2O}(°C)=20.6-4.34\ (\delta^{18}O_{CO3(VPDB)}-\delta^{18}O_{H2O(VSMOW)})$	Grossmann and Ku (1986)
Ostracods (*Ilyocypris binocularis*)	Calcite carapace	$T_{H2O}(°C)=16.2-4.2(\delta^{18}O_C-\delta^{18}O_W)+0.13*(\delta^{18}O_C-\delta^{18}O_W)^2$	Epstein et al. (1953)
Fish otoliths aragonite (*Tinca micropygoptera*)	Aragonite	$T_{H2O}(°C)=(18.654/((\ln(((10^3+\delta^{18}O_{CO3(VSMOW)})/(10^3+\delta^{18}O_{H2O(VSMOW)})))*10^3)+33.491))-273.15$	Patterson et al. (1993)
		$MAT(°C)=(\delta^{18}O_{H2O}+14.178)/0.442$ mean annual air temperature (MAT)	$\delta^{18}O_{H2O}$ from the NISOT (National Isotope Network of Switzerland)

teeth *T. micropygoptera*: $T_{H2O}=17.1\pm2.7$ °C) and benthic organisms (ostracod valves: *I. binocularis*: $T_{H2O}=16.7\pm5.0$ °C) give similar mean T_{H2O} of around +17 °C. The T_{H2O} calculated from the gastropod shells of *Gyraulus* spp. ($T_{H2O}=20.6\pm5.6$ °C), that lived in the charophyte girdle of the lake littoral zone, is about 4 °C higher, in accordance with a shallower water depth. Otoliths from *T. micropygoptera* ($T_{H2O}=21.8\pm1.4$ °C) yield the highest water temperature, probably representing the warmest months of the growing season (Grimes et al., 2003), during which fish otoliths are known to grow most rapidly (e.g., Patterson et al., 1993). The T_{H2O} of around 17 °C calculated from the fish teeth of *T. micropygoptera* probably best represents the mean T_{H2O} of the lake water as fish migrate through the water column.

Calculated T_{H2O} most likely represent those of the littoral or slope zone as the lake in the Steinheim basin was a deep, meromictic lake with episodic oxygen deficient, hostile conditions in the hypolimnion (e.g., Mensink, 1984).

5.4. Calculation of mammal drinking water $\delta^{18}O_{H2O}$ values and MAT

Using existing species-specific $\delta^{18}O_{PO4}$–$\delta^{18}O_{H2O}$ calibrations for extant large mammal taxa (equids, proboscideans, suids, cervids, rhinocerotids; Table 14) a drinking water $\delta^{18}O_{H2O}$ value of -5.9 ± 1.7‰ VSMOW ($n=31$) can be determined from the enamel $\delta^{18}O_{PO4}$ values of their teeth. This $\delta^{18}O_{H2O}$ value is similar to that calculated for the enamel of large mammal teeth from other Miocene localities of the nearby Molasse basin (Tütken and Vennemann, 2005) and is therefore assumed to be representative of the isotopic composition of the local meteoric water in the region of southern Germany/Switzerland at that time. The $\delta^{18}O_{H2O}$ value of −6‰ is about 4‰ higher than that of groundwater from the Steinheim basin today ($\delta^{18}O_{H2O}=-9.9\pm0.3$, $n=7$, Table 15), suggesting a much warmer climate during the Middle Miocene. Because the $\delta^{18}O_{H2O}$ values of precipitation are positively correlated with the mean annual air temperature (MAT), especially in mid to high latitudes (Dansgaard, 1964; Rozanski et al., 1993), they are a valuable climate proxy. Using a $\delta^{18}O_{H2O}$-MAT regression (Eq. (2)) based on present-day precipitation and air temperature data from the National Isotope measurement network of Switzerland (NISOT) (unpublished NISOT data; Schürch et al., 2003), a MAT of 18.8 ±3.8 °C (Fig. 8) can be calculated from the $\delta^{18}O_{H2O}$ value of -5.9 ± 1.7‰.

$$MAT(°C) = (\delta^{18}O_{H2O} + 14.178)/0.442 \quad (2)$$

For the $\delta^{18}O_{PO4}$–$\delta^{18}O_{H2O}$ calibration of rodents Eq. (3) as given by Grimes et al. (2003), drinking water $\delta^{18}O_{H2O}$ values for all the small mammal teeth from the Steinheim basin were calculated to cover a range from −3.1 to +12.3‰ (Fig. 7). These $\delta^{18}O_{H2O}$ values indicate ingestion of highly ^{18}O-enriched water by some of the small mammals. Similar $\delta^{18}O_{H2O}$ values of up to 12‰,

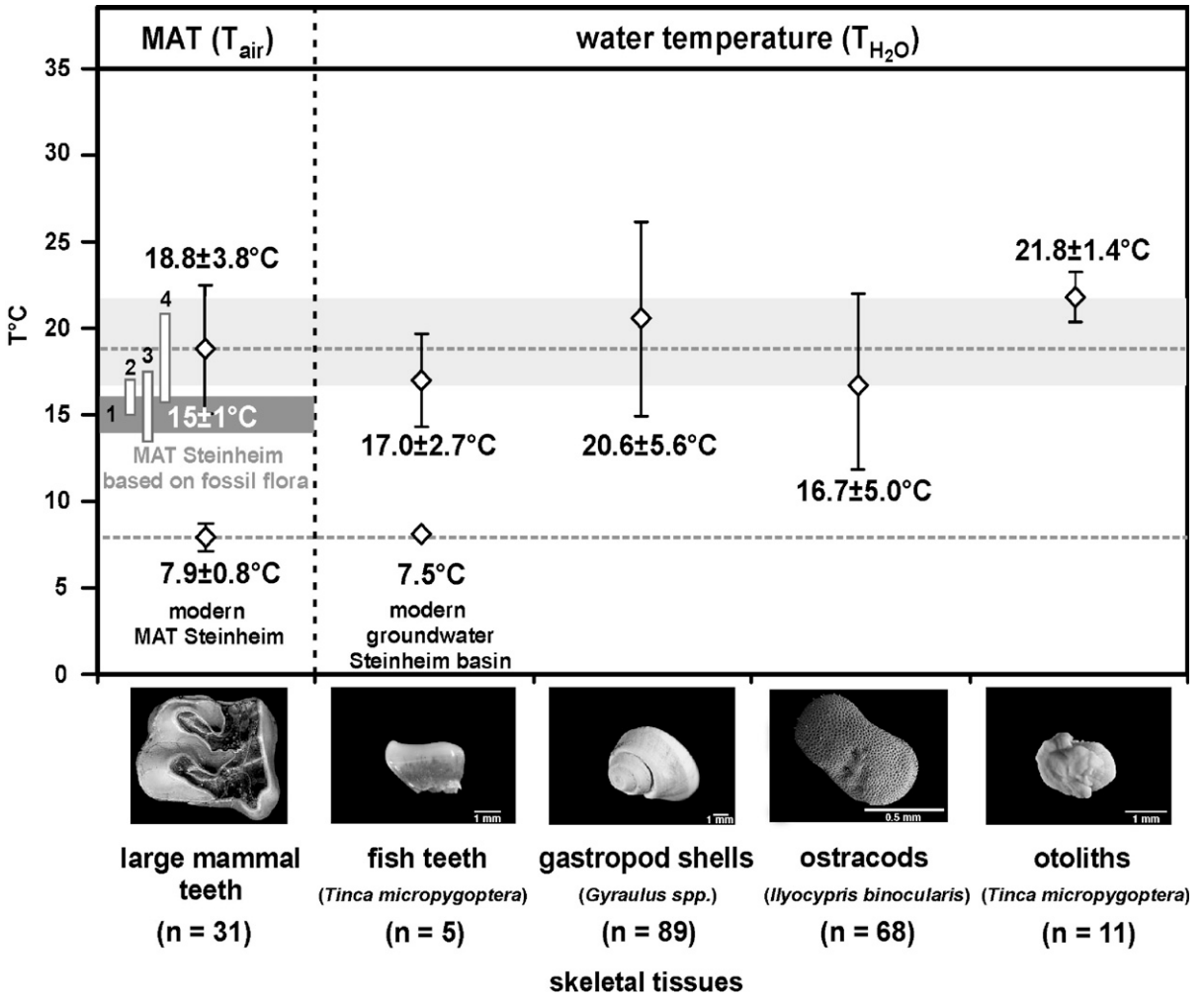

Fig. 8. Palaeolake water temperatures (T_{H2O}) for the Steinheim basin calculated from the $\delta^{18}O$ values of phosphatic and carbonaceous skeletal remains of aquatic vertebrates and invertebrates. The temperature equations for T_{H2O} calculations from phosphatic fish teeth, aragonitic freshwater gastropod shells, calcitic ostracod valves, and otoliths are given in Table 14. The lake water $\delta^{18}O_{H2O}$ value was assumed to be +2‰ as reconstructed from aquatic turtle bone $\delta^{18}O_{PO4}$ values (c.f. Table 14). The mean annual air temperature (MAT) was calculated with a modified Dansgaard equation (Table 14) from the mean $\delta^{18}O_{H2O}$ value derived from enamel of large mammal teeth (Fig. 7), representing the Middle Miocene meteoric water value. For comparison are plotted: present-day MAT and groundwater T_{H2O} for the Steinheim basin, and MATs based on the fossil flora from 1: Steinheim basin (Gregor, 1983) and other contemporaneous localities, 2: Adelegg, (Eberhard, 1989), 3: Wengen (Eberhard, 1989), 4: Rhine Basin brown coal pit Zukunft/Mine 6D (Utescher et al., 2000).

also with a positively skewed distribution, were calculated from Eocene rodent enamel (Grimes et al., 2003).

$$\delta^{18}O_{H2O} = [(\delta^{18}O_{PO4} - 17.42) - 0.24]/0.59 \quad (3)$$

Calculating a log-normal mean drinking water $\delta^{18}O_{H2O}$ value (following Grimes et al., 2005) for the pikas and rodents separately, $\delta^{18}O_{H2O}$ values of +2.7± 2.3‰ (n=7), respectively +6.3±2.3‰ (n=5) are obtained. Thus, the small mammal teeth from the Steinheim basin do not faithfully record the meteoric water ($\delta^{18}O_{H2O} \sim -6$‰) as inferred from the large mammal teeth but instead reflect intake of water from a ^{18}O-enriched local water source and/or plant water. However, these $\delta^{18}O_{H2O}$ results for small mammal teeth might be biased to some degree due to methodological differences to the approach of Grimes et al. (2003, 2005): 1) whole teeth instead of enamel were used, which may be influenced by diagenesis (see Section 5.1); 2) rodent incisor teeth instead of molar teeth were analysed and according to Lindars et al. (2001) modern rodents show a large intra-jaw variability of $\delta^{18}O$ values and they recommend the use of teeth formed late during

Table 15
$\delta^{13}C$ (DIC) and $\delta^{18}O_{H2O}$ values of water samples from the Steinheim basin and the surrounding

Name	Type of karst water source	Locality	Date of collection	DIC $\delta^{13}C$ VPDB	σ	$\delta^{18}O_{H2O}$ VSMOW	σ
Remsursprung	River source		19.03.2005	−14.4	0.03	−10.6	0.07
Pfefferquelle	River source	Königsbronn, Swabian Alb	19.03.2005	−17.2	0.06	−11.5	0.08
Brenztopf	River source	Königsbronn, Swabian Alb	19.03.2005			−10.5	0.05
Schwarzer Kocher Quelle	River source	Unterkochen, Swabian Alb	19.03.2005	−16.1	0.02	−10.8	0.05
Schwarzer Kocher Quelle	River source	Unterkochen, Swabian Alb	19.03.2005	−16.9	0.04	−11.4	0.04
Weisser Kocher Quelle	River source	Unterkochen, Swabian Alb	19.03.2005	−17.5	0.04	−10.6	0.05
Hülbe am Stockbrunnen	Pond	Steinheim basin	08.06.2005			−6.7	0.07
Brunnen in Sontheim	Groundwater well	Water works Steinheim Basin	08.06.2005	−14.2	0.03	−10.4	0.08
Lettenhülbe	Pond	Steinheim basin	08.06.2005	−9.6	0.09		
Kesselhülbe	Pond	Steinheim basin	08.06.2005			−8.8	0.07
Eschentalbrunnen	Groundwater well	Steinheim basin	08.06.2005	−14.8	0.03	−10.0	0.07
Brunnen im Hirschtal	Groundwater well	Steinheim basin	06.06.2005	−15.6	0.04	−10.2	0.05
Rohrbrunnen	Groundwater well	Steinheim basin	06.06.2005	−16.0	0.04	−9.8	0.07
Hülbe	Pond	Steinheim basin	03.06.2005	−7.5	0.08		
Doppelhülben	Pond	Steinheim basin	03.06.2005	−16.5	0.05	−8.6	0.07
Feldhülbe	Pond	Steinheim basin	03.06.2005	−17.8	0.04	−8.7	0.07
Hülbe	Pond	Steinheim basin	03.06.2005	−7.5	0.10		
Schuleneshülbe	Pond	Steinheim basin	03.06.2005	−15.0	0.05	−7.5	0.08
Türkenbrunnen	Groundwater well	Steinheim basin	03.06.2005			−10.0	0.07
Linsenbrunnen	Groundwater well	Steinheim basin	03.06.2005	−14.7	0.03	−10.2	0.07
Klosterhofbrunnen	Groundwater well	Steinheim basin	08.06.2005	−15.9	0.04	−9.6	0.07

ontogenesis, such as third molar teeth. However, their study did not include incisor teeth; 3) the rodent species-specific Eq. (3) is based only on results for the wood mouse *Apodemus sylvaticus* (Luz et al., 1984). Because rodent incisors were analysed, the rodent species could not be determined and thus no information about their feeding and drinking behaviour is available. For the pikas the rodent equation was assumed to be valid though their drinking behaviour/metabolism might have been different. Despite these uncertainties, it seems unlikely that the large difference of >8‰ between reconstructed small and large mammal mean drinking water $\delta^{18}O_{H2O}$ values are caused by these methodological differences.

5.5. Differences in the drinking behaviour of small and large mammals

Compared to the enamel of large mammal teeth ($\delta^{18}O_{PO4}$=18.1±1.5‰, n=31) the small mammal (*G. socialis*, *P. oeningensis*, rodents indet.) teeth ($\delta^{18}O_{PO4}$= 20.5±3.0‰, n=14) have a 2.4‰ higher $\delta^{18}O_{PO4}$ value and a two times larger standard deviation. This supports a stronger evaporative influence on the body water of the small mammals, which might be related either to ingestion of ^{18}O-enriched drinking water, ^{18}O-enriched moisture from the food, and/or related to physiological oxygen isotope fractionation due to a small body mass and high metabolic rate (e.g., Bryant and Froelich, 1995; however, see also Section 5.4. above).

Using the data obtained for the pikas and rodents from the Steinheim basin separately, the teeth from the pika *P. oeningensis* ($\delta^{18}O_{PO4}$=19.5±3.0‰, n=7) have about 2‰ lower $\delta^{18}O_{PO4}$ values than the rodent teeth ($\delta^{18}O_{PO4}$=21.6±3.3‰, n=5). The pikas thus ingested the majority of their body water oxygen from a less evaporated water source than the rodents, which possibly ingested more water from feeding than from drinking. The metabolism and drinking behaviour of the extinct pika *P. oeningensis*, which is the most abundant mammal fossil in the Steinheim basin (Heizmann and Reiff, 2002), is unknown. However, it lived in the more humid, vegetation-rich area directly surrounding the lake (Heizmann and Fahlbusch, 1983), supporting a water-related lifestyle and making the use of lake water likely. This is supported by the log-normal mean drinking water $\delta^{18}O_{H2O}$ value of +2.7±2.3‰ for the pikas, which is close to that estimated for the lake water as reconstructed from the aquatic turtle bones (Fig. 7). Small mammals, especially pikas, with much smaller home ranges were thus presumably dependent on the ^{18}O-enriched lake in the Steinheim basin as the drinking water source.

$\delta^{18}O_{H2O}$ values for large mammals are about 8‰ lower than those calculated for the lake water using aquatic turtle bones. Therefore, the large mammals did not use the lake water as a principal drinking water

source, even though other surface water sources may have been scarce on the surrounding karstic limestone plateau of the Swabian Alb (Fig. 1). Sympatric large and small mammal teeth from the same autochthonous fossil assemblage of the Steinheim basin thus record different drinking water oxygen isotopic compositions. It is clear that despite the availability of the ^{18}O-enriched water body of Lake Steinheim, large mammals mostly drank meteoric water from other surface water sources with lower $\delta^{18}O_{H2O}$ values. Several possible explanations may account for this: (1) poor water quality (high salinity?) as a result of extensive evaporation, (2) mammals drank from ground or surface water entering the lake, as observed close to the salt lakes in the East African rift valley today (Heissig, pers. comm., 2005), (3) the large mammals were migratory.

Concerning point (1) it is known that large mammals are sensitive to water quality deterioriation such as elevated ion contents and they migrate to avoid such waters sources (e.g., Wolanski et al., 1999). Saline conditions prevailed most of the time in the contemporaneous shallow water long-term lake of the nearby Nördlinger Ries (Wolff and Füchtbauer, 1976; Rothe and Hoefs, 1977; Jankowski, 1981). But in contrast to the Nördlinger Ries, for Lake Steinheim there is no direct evidence for saline or brackish water conditions. The abundance of freshwater species (charophytes, gastropods, ostracods, fresh water turtles and fish) within Lake Steinheim (Gorthner, 1992; Janz, 1992; Schweigert, 1993; Janz, 1997; Schudack and Janz, 1997) during the *trochiformis* and lower *oxystoma* period, that is the period corresponding to the main deposits of the mammal remains (Fig. 2), would not support a high water salinity. Nevertheless, the low-diversity of the fish and post-*kleini* period ostracod fauna (Gaudant, 1989; Janz, 1992, 1997) can be taken to support restrained living conditions. Furthermore, geochemical investigations also support large changes of the dissolved ion content of the lake water due to evaporation (Bajor, 1965).

With regard to explanation (2), no major fluviatile inflow into the Steinheim basin is known and the ground water level in a karst landscape is generally well below the surface. Thus, this possibility is considered unlikely. This leads to explanation (3). Many large mammals have large home ranges thus access to different surface waters. Therefore, the large mammals from the Steinheim basin may well have used water sources located in the Molasse basin just south of the Swabian Alb. At the time of the Ries impact the North Alpine Foreland basin formed a system of large longitudinal streams that accumulated gravels, sands, and silts of the Upper Freshwater Molasse (Böhme et al., 2001), suggesting the presence of other surface water sources. This possibility of extensive migration away from the Swabian Alb plateau will be considered more closely using Sr isotopic compositions of the mammalian tooth enamel.

5.6. Sr isotope compositions of mammal teeth — migration or local Sr uptake?

The Sr isotopic composition of skeletal apatite of mammal bones and teeth reflects that of the water and food ingested, with the latter being the principal Sr source. Because of the small mass difference of the two stable Sr isotopes used, ^{87}Sr and ^{86}Sr, no measurable fractionations of the $^{87}Sr/^{86}Sr$ ratio occurs during weathering or sedimentation processes, nor during metabolism or tissue mineralization in the plant or animal. Therefore, the $^{87}Sr/^{86}Sr$ ratio does not change along the food chain (e.g., Blum et al., 2000) and $^{87}Sr/^{86}Sr$ ratios of biological tissues reflects the Sr isotopic composition of the biologically-available Sr entering the food web which is in most cases closely related to that of the bedrock geology (Graustein, 1989; Price et al., 2002). In settings where the $^{87}Sr/^{86}Sr$ ratios of the underlying rock formations differ significantly and are well constrained, the $^{87}Sr/^{86}Sr$ ratio can be used as isotopic fingerprint for migration movements of animals or human beings between different geologic, respectively Sr isotopic domains (Sillen et al., 1998; Hoppe et al., 1999; Müller et al., 2003). Possible migration and thus potential use of food and water sources other than those in the vicinity of the Steinheim basin would be supported by tooth enamel $^{87}Sr/^{86}Sr$ values that are different from the expected $^{87}Sr/^{86}Sr$ values of the Swabian Alb plateau carbonates.

The Steinheim basin is situated on the Swabian Alb plateau made up of Upper Jurassic marine limestones (Fig. 1). The Sr isotopic composition of the carbonates is well known ($^{87}Sr/^{86}Sr = 0.70697$ to 0.70722, McArthur et al., 2001). Sr isotopic analysis from Upper Jurassic limestones of the Swabian Alb yield $^{87}Sr/^{86}Sr$ ratios of 0.7071 to 0.7072, falling in that range (Fig. 9). Such $^{87}Sr/^{86}Sr$ ratios are expected to be incorporated in skeletal tissues of animals feeding on the Swabian Alb plateau as carbonates readily dissolve and are rich in Sr (Bausch, 1965).

Of the 11 large mammal fossil enamel samples analysed from the Steinheim basin only one sample from the equid *Anchitherium* ($^{87}Sr/^{86}Sr = 0.707027$) has a $^{87}Sr/^{86}Sr$ value typical for the Upper Jurassic limestone (Fig. 9). All other enamel samples have

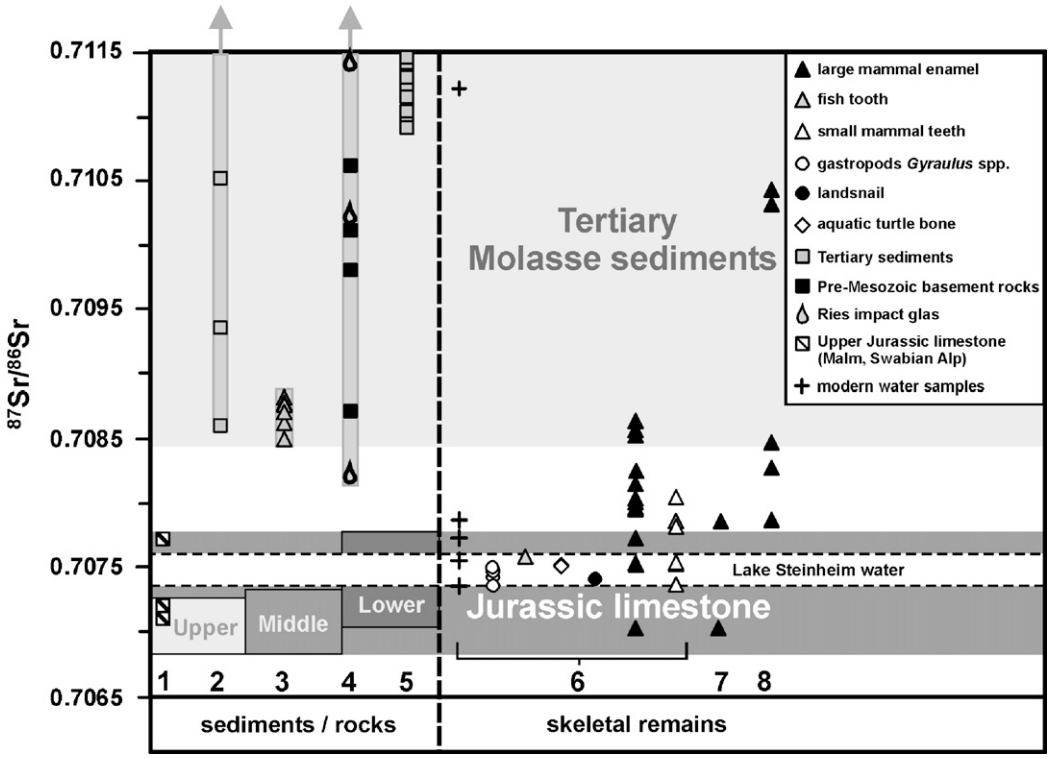

Fig. 9. Plot of the Sr isotopic compositions of analysed skeletal remains from the Steinheim basin (6), the Molasse basin (8), and the Nördlinger Ries (7). For comparison the $^{87}Sr/^{86}Sr$ data from underlying rocks and sediments of surrounding areas are given: (1) Upper Jurassic limestone from the Swabian Alb after Horn et al. (1985), Pache et al. (2001), (2) Molasse sediments after Vennemann, unpublished data, (3) shark teeth from Molasse sediments after Vennemann and Hegner (1998), (4) crystalline basement rocks from Nördlinger Ries after Schnetzler et al. (1969), Horn et al. (1985) and (5) Tertiary freshwater carbonates from the Ries after Pache et al. (2001). The $^{87}Sr/^{86}Sr$ ranges for Jurassic limestone and Molasse sediments are shaded in grey after McArthur et al. (2001), respectively, Bentley and Knipper (2005) and references therein. Lower, middle and upper Jurassic limestone ranges are marked. The white bar represents the range of the lake water $^{87}Sr/^{86}Sr$ ratios derived from aragonitic *Gyraulus* gastropod shells and aquatic vertebrate skeletal remains.

$^{87}Sr/^{86}Sr$ values >0.70753 that are higher than those for marine Jurassic carbonates and the lake water ($^{87}Sr/^{86}Sr$ about 0.70743) but similar to those of Tertiary Molasse sediments (Fig. 9). It is possible that the Upper Jurassic limestone of the Swabian Alb was, in parts, covered by Tertiary sediments with higher $^{87}Sr/^{86}Sr$ ratios than the underlying Upper Jurassic limestone. Thus, the Sr entering the food chain may represent a mixture of more radiogenic sediment-derived and less radiogenic limestone-derived Sr. A Tertiary sediment cover is today largely restricted to the southern margin of the Alb, bordering the Molasse basin which was deposited during the Early to Middle Miocene marine transgression of the Upper Marine Molasse and the following basal part of the Upper Freshwater Molasse (Geyer and Gwinner, 1991, Fig. 2a). Small patches of Tertiary sediments also existed on the Swabian Alb plateau at least in the Ries area at the time of the meteorite impact (Horn et al., 1985; Engelhardt et al., 1987; Vennemann et al., 2001). The ejecta of the Ries impact themselves (Fig. 1) are mostly made up of Upper Jurassic limestone and thus not of relevance.

The region north of the Swabian Alb consists of Mesozoic rocks, mainly Triassic lime-, clay-, and sandstones with high $^{87}Sr/^{86}Sr$ ratios of 0.708 to 0.714 (Horwarth, 2000), while in the south the Tertiary Molasse basin sediments occur (Fig. 1) with $^{87}Sr/^{86}Sr \geq 0.7085$ (Schnetzler et al., 1969; Bentley and Knipper, 2005). The enamel of most large mammal teeth from the Steinheim basin have $^{87}Sr/^{86}Sr$ ratios between those of the Jurassic limestone and the Tertiary Molasse basin sediments and three of them, two *Gomphotherium* and one *Palaeomeryx* teeth, have $^{87}Sr/^{86}Sr$ ratios ≥ 0.7085 and fall in the $^{87}Sr/^{86}Sr$ range of the Molasse sediments (Fig. 9). This would support migration between the Swabian Alb and the Molasse basin for which the northern boundary lies about 30 km south of the Steinheim basin (Fig. 1). The migration of gomphotheres over such a distance is very likely as proboscideans are capable of large, seasonal migration of up to 500 km as,

for example, established for Quaternary mastodonts (Hoppe et al., 1999) and modern elephants in Africa.

A third possibility to account for the Sr isotope variations is the local uptake of high $^{87}Sr/^{86}Sr$ food and water sources. The central hill mainly consists of disturbed Middle Jurassic clay and siltstones that are potential sources for radiogenic Sr with much higher $^{87}Sr/^{86}Sr$ ratios than the surrounding Upper Jurassic limestone, as clearly indicated by a modern surface water sample ($^{87}Sr/^{86}Sr$ = of 0.71122, Fig. 9) taken from a little pond situated on the central hill. When the central hill fell dry it became probably land-connected and was inhabited by mammals and other land vertebrates (Heizmann, 1973). At least some of the large mammals may, therefore, have lived on the central hill and taken up some radiogenic Sr there. But the low $\delta^{18}O_{H2O}$ values calculated from the enamel indicates that they could not have lived there permanently because in this case they would have relied on the ^{18}O-enriched lake water ($\delta^{18}O_{H2O}$ = +2.0‰) as drinking water source too.

Teeth of small mammals with much smaller home ranges and that most likely took up their food and water in the local surrounding of the lake, have similar $^{87}Sr/^{86}Sr$ ratios as the enamel of most large mammals (Fig. 9). This is surprising but is also compatible with the measurements of modern groundwaters from the Steinheim basin (Fig. 9), that equally indicate that the $^{87}Sr/^{86}Sr$ of groundwaters may in fact not have been controlled only by the Jurassic marine carbonates. Thus, it has been possible for small mammals to ingest Sr with $^{87}Sr/^{86}Sr$ ratios as high as 0.7081 locally, though some were brought there by birds of prey as indicated by in situ found owl pellets material (Heizmann and Reiff, 2002). The combined interpretation of the Sr and the oxygen isotope compositions of the large mammals, however, supports migrational movements >30 km at least for some of the large mammals.

5.7. $\delta^{13}C$ values of mammal teeth — feeding in a C_3 plant dominated ecosystem

The C_3 and C_4 photosynthetic pathways fractionate carbon isotopes to different degrees, hence C_3 and C_4 plants have $\delta^{13}C$ values ranging from about −30 to −22‰ and −14 to −10‰, respectively (e.g., Deines, 1980; Farquhar et al., 1989). For large herbivorous mammals the enamel $\delta^{13}C$ values reflect those of the food with an offset of about 14‰ (Cerling and Harris, 1999), and thus may record the proportion of C_3/C_4 plants in mammalian diet (e.g., Quade et al., 1992; Cerling et al., 1997; Cerling and Harris, 1999). The mean enamel $\delta^{13}C$ value of −11.1 ± 1.1‰ (n = 40) of the large herbivorous mammals indicates that they exclusively fed on C_3 plants. Thus, the surrounding of the Steinheim basin was covered by C_3 vegetation and there is no evidence for the occurrence of C_4 plants. This is in good agreement with the fact that a global C_4 plant dispersal is only recorded from the late Miocene (8 to 6 Ma) onwards (Cerling et al., 1997). A similar mean enamel $\delta^{13}C$ value of −10.9 ± 1.2‰ (n = 270) of Miocene mammal teeth from the nearby Molasse basin further corroborates a C_3 plant dominated ecosystem in this area (Tütken and Vennemann, 2005).

5.8. $\delta^{13}C$ values of the biogenic carbonates — changes in carbon cycling and lake level fluctuations

Respiration by C_3 plants and/or natural decomposition of this type of organic matter in the soil produces CO_2 with similar $\delta^{13}C$ values compared to the original vegetation itself, but the diffusion of this CO_2 through the soil leads to an enrichment of about 4‰ (e.g., Cerling et al., 1991). For most natural systems, this soil CO_2 is the major source of dissolved inorganic carbon (DIC) in groundwaters. At typical temperature and pH conditions for temperate climate zones (about 15 °C and pH about 7), equilibrium dissolution of soil CO_2 would produce DIC with $\delta^{13}C$ values of about −15 to −16‰ (Mook et al., 1974). Such values have been measured for the present-day groundwaters ($\delta^{13}C_{DIC}$ = −15.2 ± 0.7‰, n = 6, Table 15) in the vicinity of the Steinheim basin. Given ε(calcite-DIC) of about +2 to +3‰ (Mook et al., 1974; Zeebe et al., 1999), a $\delta^{13}C$ value for carbonates of −14 to −12‰ would be expected, if precipitated in equilibrium with groundwaters dominated by typical C_3 plant derived soil-CO_2. However, the biogenic carbonates of gastropod and ostracod shells of the Steinheim basin have much higher $\delta^{13}C$ values (Fig. 5).

Several investigations so far have shown that molluscs precipitate their shell carbonate in isotopic equilibrium with the ambient water (e.g., Epstein et al., 1953; Fritz and Poplawski, 1974; Grossmann and Ku, 1986) and thus the $\delta^{13}C$ value of shell carbonate should reflect that of DIC. In contrast, a recent study monitoring different live freshwater gastropods and their host springs with nearly constant temperature and isotopic composition indicates that offsets from expected isotopic equilibrium shell $\delta^{13}C$ values, so called vital effects attributed to the incorporation of metabolic carbon enriched in ^{12}C, of up to 4‰ can occur due to behavioural and physiologic differences (Shanahan et al., 2005 and refs therein). Therefore, vital effects may lower shell carbonate $\delta^{13}C$ values relative to

equilibrium values expected. Such vital effects seem to be responsible for the low $\delta^{13}C$ values of the *T. micropygoptera* otoliths ($\delta^{13}C = -11.6 \pm 1.1‰$, $n = 12$) (Fig. 5). The high $\delta^{13}C$ values of the aragonitic *Gyraulus* spp. gastropod shells and the calcitic *I. binocularis* ostracod valves may thus be taken as minimum estimates for the $\delta^{13}C_{DIC}$ of the palaeolake water. Even higher $\delta^{13}C_{DIC}$ values around +3.5‰ can be inferred from characean stem fragments and carbonate sediment particles (Fig. 5).

High $\delta^{13}C_{DIC}$ values in shallower groundwaters or surface waters can be caused by isotopic exchange with or dissolution of atmospheric CO_2 (e.g., Talbot, 1990). This becomes particularly important in evaporatively influenced water bodies such as long-term lakes (Talbot, 1990) or in seawater. In addition, weathering and dissolution of carbonates in aquifers may strongly influence the $\delta^{13}C$ values of DIC, commonly leading to an increase in ^{13}C (e.g., Yang et al., 1996). Finally, primary bioproductivity in the water column will tend to increase the $\delta^{13}C_{DIC}$ value, as ^{12}C is preferentially incorporated into the biological tissues (e.g., Kroopnick et al., 1972; Longinelli and Edmond, 1983; Farquhar et al., 1989).

Over the complete sediment section from the basal *kleini* to the terminal *supremus* beds, the $\delta^{13}C$ values of both aragonitic gastropod shells and calcitic ostracod valves are similar and co-vary (Fig. 4). Their $\delta^{13}C$ values increase discontinuously and parallel the long-term lake level fluctuations with two transgressive–regressive cycles established from sedimentological data (Mensink, 1984; Bahrig et al., 1986; see Fig. 4). This suggests that carbon cycling and lake level fluctuations appear to be linked.

That the high $\delta^{13}C$ values are caused by unusually high bioproductivity in the water of Lake Steinheim is considered unlikely, even though a dense characean vegetation existed in the littoral zone (Schweigert, 1993). Biologic activity may well influence the $\delta^{13}C_{DIC}$ values by several permille, but much of this biologically fixed and thus isotopically-light carbon is returned to the system during respiration and/or oxidation of organic matter (e.g., Wachniew and Różański, 1997). The Steinheim basin sediments are not very rich in organic matter and the lake is largely considered to have been oligotrophic (Schweigert, 1993), indicating that primary bioproductivity is unlikely to have caused the high $\delta^{13}C_{DIC}$ values of lake waters. A substantial input of terrestrial organic material to the lake, as indicated by sediments richer in fossil land plant remains, is predominantly associated with low-stand periods of the lake level for the *kleini*/lower *steinheimensis* and the *oxystoma* period (Schweigert, 1993). These sediments also have the lowest $\delta^{13}C$ values for the biogenic carbonates (Fig. 4), supporting additional input of carbon from oxidized terrestrial organic matter to the carbon budget of the lake during these periods. But the high $\delta^{13}C$ values coupled with the increase in values throughout the section (Fig. 4) indicate that the lake water DIC was probably largely controlled by exchange with atmospheric CO_2 (e.g., Craig, 1953; Bajor, 1965; Talbot, 1990) and less influenced by soil-zone CO_2. Increased inflow of groundwater with DIC controlled by the dissolution of marine Jurassic limestones with high $\delta^{13}C_{DIC}$ values (Fig. 5) is not likely, given the present-day values for groundwater ($\delta^{13}C_{DIC} = -15.2 \pm 0.7‰$, $n = 6$, Table 15) that essentially passes through the same type of aquifer material.

5.9. Sr isotope compositions of aragonitic Gyraulus shells — a record of long-term lake level fluctuations?

The Sr isotopic composition of river and lake water reflects that of the rocks weathering in the drainage area and varies only if the geology and/or hydrology of the drainage area changes significantly (Jones and Faure, 1978; Neat et al., 1979; Hart et al., 2004). Therefore, the Sr isotopic composition of biogenic carbonates from aquatic organisms is a valuable tool for the reconstruction of lake level fluctuations (Hart et al., 2004). Because all investigated *Gyraulus* spp. shells have preserved their original aragonitic mineralogy, they should faithfully record the lake water $^{87}Sr/^{86}Sr$ ratio at the time of mineralisation. The Sr isotopic composition of the *Gyraulus* shells from all 7 gastropod beds varies close to a mean $^{87}Sr/^{86}Sr$ ratio of 0.70743 ± 0.00004 ($n = 10$) but there are subtle but significant changes of the $^{87}Sr/^{86}Sr$ ratios that are positively correlated with known lake level fluctuations (Fig. 4). Lake level fluctuations for the Steinheim basin are mainly ascribed to tectonic movements of the Swabian Alb and resulting changes of the groundwater level (Reiff, 1988) though evaporation may have played an additional role (Bajor, 1965, this study). If the lake level fluctuations would be due to intensified evaporation only no changes of the lake water $^{87}Sr/^{86}Sr$ ratio are to be expected. During tectonically induced movements of the groundwater level the water balance of the lake is likely to change. Thus, if the Steinheim basin was a groundwater window lake, during transgressive phases a stronger groundwater inflow with a slightly more radiogenic $^{87}Sr/^{86}Sr$ ratio is to be expected, taking the present-day groundwater Sr isotopic composition ($^{87}Sr/^{86}Sr$ about 0.7076 ± 0.0002, $n = 4$) of the Steinheim basin as valid for the Middle

Miocene. Assuming that during lake level low-stand phases precipitation rate and surface runoff stay constant, a higher proportion of Sr will be derived from surface runoff than from groundwater inflow, supplying slightly less radiogenic Sr from the dissolution of the surrounding Upper Jurassic limestone ($^{87}Sr/^{86}Sr \leq 0.7072$, Fig. 4). Such a scenario would be compatible with the results summarized in Fig. 4.

It is interesting to note that the Sr isotopic composition of one *T. micropygoptera* fish tooth and two aquatic turtle bones have significantly higher $^{87}Sr/^{86}Sr$ ratios of ≥ 0.705 than the aragonitic *Gyraulus* spp. shells and *T. micropygoptera* otolith. This may indicate some diagenetic exchange of Sr from the biogenic phosphate with more radiogenic Sr from the ground water or may reflect primary small Sr isotopic compositional differences of the not so well mixed meromictic lake water body of Lake Steinheim. But the former explanation seems more likely as the turtle bone has the highest $^{87}Sr/^{86}Sr$ ratio and bone can relatively quickly alter its Sr isotopic composition (Price et al., 2002 and references therein). Furthermore, the aragonitic *T. micropygoptera* otolith still has the same $^{87}Sr/^{86}Sr$ ratio as the lake water ($^{87}Sr/^{86}Sr \sim 0.7043$) while the *Tinca* tooth has a higher $^{87}Sr/^{86}Sr$ ratio of 0.70514 (Fig. 4).

5.10. Palaeoclimatic and palaeoenvironmental reconstruction for the Steinheim basin

In Section 5.3 mean water temperatures for the lake in the Steinheim basin have been reconstructed from the different aquatic proxies to range from 16.7 to 21.8 °C with these temperatures reflecting the different habitats and/or growing seasons of the species used. This temperature range also overlaps within error with the MAT of 18.8±3.8 °C calculated from the mean $\delta^{18}O_{H2O}$ value derived from enamel of the large mammals (Fig. 8). The good agreement between MAT and T_{H2O} confirms the validity of the calculated palaeotemperatures as MAT and lake surface T_{H2O} are often closely correlated (e.g., Livingstone and Lotter, 1998). Such a correlation is also apparent between the modern day groundwater temperature (T_{H2O}=7.5 °C) and the MAT (7.9±0.8 °C, n=28) in the Steinheim basin (Seidel, pers. comm. 2005, Fig. 8). Thus, groundwater recharge T_{H2O} is likely to have been similar to MAT for the Middle Miocene Lake Steinheim.

The Middle Miocene MAT of 18.8 °C is about 11 °C warmer than the present-day MAT of 7.9 in the Steinheim basin (Fig. 8). The MAT estimates from the contemporaneous Middle Miocene fossil floras from the Steinheim basin itself (15±1 °C, Gregor, 1983) and other localities in SW Germany (Adelegg: 16±1 °C; Wengen: 15.5±2 °C, Eberhard, 1989) yield 3 to 4 °C lower MATs (Fig. 8). In contrast, our reconstructed MAT fits well into the MAT range of 15.5 to 21.0 °C reconstructed for the late Early to late Middle Miocene based on fossil megafloras from brown coal pits in NW Germany (Utescher et al., 2000, Fig. 8) and to the sea surface temperature of the North Sea at that time (Buchard, 1978). Furthermore, the reconstructed MAT is in accordance with the occurrence of warmstenotherm ostracods in the lake sediments (Janz, 1997) such as *Cyprinotus inaequalis*, indicative of a MAT ≥20 °C (Janz, 1992). It is also in agreement with the MAT of >17.4 up to 21±1 °C MAT reconstructed for the Miocene climate optimum in Central Europe (18 to 14 Ma) based on the occurrence of thermophilic vertebrate taxa (Böhme, 2003). However, a significant decrease in MAT down to values of 15 to 16 °C occurred between 14.0 and 13.5 Ma (Böhme, 2003), related to global cooling (e.g., Zachos et al., 2001). If the estimated age of 13.5 Ma for the mammal-bearing lake sediments of the Steinheim basin is correct, our data would suggest that a warm-temperate climate with a MAT around 19±4 °C still prevailed in the region of the Steinheim basin until then. The high $\delta^{18}O$ values of around +2‰ for the lake waters of the Steinheim basin and Nördlinger Ries (this study, Pache et al., 2001) also suggest a significant evaporation during this period (Bajor, 1965; Rothe and Hoefs, 1977; this study). Whether this evaporation occurred under conditions of high or low humidity is more difficult to establish. Based on palaeofloral evidence a warm-temperate, seasonal, semi-arid climate existed in the area around the Steinheim basin (Schweigert, 1993; Heizmann and Reiff, 2002). Semi-arid conditions are also supported by the saline condition prevailing most of the time for the nearby Nördlinger Ries Lake (Rothe and Hoefs, 1977; Jankowski, 1981). However, a change towards freshwater conditions in the upper part of the Ries Lake might indicate a climate humidification (Jankowski, 1981). According to experimental measurements, models, and measurements on recent controlled natural settings (Craig et al., 1963; Gonfiantini, 1986), at high humidities (≥75%) many lakes subjected to evaporation rapidly reach a maximum, limiting value of isotopic enrichment and then remain practically constant in value, irrespective of the initial $\delta^{18}O$ values of water (Gonfiantini, 1986). The latter constancy represents a steady-state between inflow and evaporation during the evaporative stages. This is in contrast to evaporative systems at low humidities, where the $\delta^{18}O$ of water continues to change as a function of the extent of

evaporation. As such, the rapid change from much lower $\delta^{18}O$ values during the *kleini* period to higher but more or less constant $\delta^{18}O$ values in the whole post-*kleini* period would support evaporation at high humidities for the Lake Steinheim. A similar trend is also recorded in the lake sediments of the Nördlinger Ries (Rothe and Hoefs, 1977). High humidity is further supported by high annual precipitation rates of 1250±250 mm/a estimated from the fossil flora of the Steinheim basin and the Nördlinger Ries (Gregor, 1983) as well as other Middle Miocene localities in Germany (Eberhard, 1989; Utescher et al., 2000), which is even higher than the modern annual precipitation in the Steinheim basin of 1038±199 mm/a (n=28) (Seidel, pers. comm. 2005). However, there is some contradiction in the palaeoclimatic interpretation of the palaeoflora from the Steinheim basin. While Schweigert (1993) deduced a warm-temperate climate with a pronounced dry season, Gregor (1983), respectively Gregor in Böhme et al. (2001), postulates instead a more humid cfa-type climate with mesophytic mixed-forests. Thus, questions on the amount of rainfall remain open, even though our data are more in favour of a higher humidity.

6. Conclusions

The Middle Miocene Steinheim basin represented an isolated long-term freshwater lake whose isotopic composition of the water was significantly enriched in ^{18}O due to evaporation. Biogenic shell carbonates of calcitic ostracod valves and aragonitic gastropod shells have $\delta^{18}O$ and $\delta^{13}C$ values similar to or even more positive than marine carbonates. The $\delta^{18}O$ values of the biogenic freshwater carbonates scatter around these mean values but remain at a high level over the complete duration of the freshwater lake except for the initial lake phase. A steady-state equilibrium between groundwater inflow and evaporation of the lake water must have existed, supporting evaporation under humid conditions. The scatter of the $\delta^{18}O$ values may reflect short term variability of groundwater inflow and evaporation under a warm climate but does not correlate with the long-term lake level fluctuations.

In contrast, $\delta^{13}C$ values of ostracod and gastropod shell carbonates parallel the known long-term lake level fluctuations of the Steinheim basin, most likely representing continued exchange of lake water DIC with and increasing dominance of C sourced from atmospheric CO_2. Sr isotopic compositions of the aragonitic gastropods also appear to record the lake level fluctuations, reflecting variable inputs of groundwater inflow and surface water runoff, supplying Sr from two isotopically different sources: Upper Jurassic limestone and Upper/Middle Jurassic marl and clay stones.

Large mammal $\delta^{18}O_{PO4}$ values indicate that meteoric water had $\delta^{18}O_{H2O}$=−5.9±1.7‰, values unlike those of the lake in the Steinheim basin for which $\delta^{18}O_{H2O}$=+2.0±0.4‰ is estimated from aquatic turtle bones, or $\delta^{18}O_{H2O}$=+2.7±2.3‰ as estimated from the pika *P. oeningensis*, which had a much smaller habitat range compared to large mammals, hence probably ingesting the lake water. The oxygen isotope compositions of tooth enamel of large and small mammals from the same autochthonous fossil assemblage can thus differ largely due to different home ranges and drinking behaviour. Tooth enamel of large mammals is preferred for the reconstruction of meteoric water $\delta^{18}O_{H2O}$ values of a certain geographic region because of their larger habitat range, their integration over more surface water sources, and the smaller influence of evaporative and/or metabolic effects on their body water compared to small mammals. For small mammals it is necessary to analyse a large number of teeth in order to get reliable and meaningful oxygen isotope compositions of meteoric water.

Migration of large mammals is also supported by the Sr isotopic composition of their tooth enamel that exceeds the range of $^{87}Sr/^{86}Sr$ for teeth of small mammals, the Steinheim basin lake, modern groundwater, and those of the Upper Jurassic limestone of the Swabian Alb. Large mammals may have migrated between the Swabian Alb plateau and the Molasse basin in the south.

During the European Neogene Mammal assemblage zone MN 7 (Middle Miocene: ~13.5 Ma), for which the Steinheim basin is the international reference locality, a MAT of 18.8±3.8 °C can be calculated using the meteoric water $\delta^{18}O_{H2O}$ value −5.9±1.7‰ derived from enamel of large mammal teeth. The reconstructed $\delta^{18}O_{H2O}$ value of +2‰ for the lake water in the Steinheim basin was used to calculate lake water temperatures (T_{H2O}) from skeletal $\delta^{18}O$ values of ostracod valves (16.7±5.0 °C), gastropod shells (20.6±5.6 °C), fish otoliths (21.8±1.4 °C) and the $\delta^{18}O_{PO4}$ value of fish teeth (17.0±2.7 °C). Fish teeth probably record best the mean lake water temperature (17.0±2.7 °C). Altogether the calculated MAT (~19 °C) and lake water temperatures (17 to 22 °C) as well as the ^{18}O-enriched lake water ($\delta^{18}O_{H2O}$=+2‰) are indicative of a warm-temperate and high-humidity climate with evaporation around the Steinheim basin during the Middle Miocene.

The presented multi-species and multi-proxy-approach combining stable C, O, and Sr isotopic compositions from skeletal remains of aquatic and terrestrial organisms allows for a differentiated palaeoenvironmental and palaeotemperature reconstruction of the aquatic freshwater ecosystem as well as of the habitat and drinking behaviour of large and small mammals.

Acknowledgements

We thank Burkhard Engesser, Naturhistorisches Museum Basel, for the permission of sampling teeth and other skeletal remains from the Steinheim basin. We are grateful to Ronald Boettcher, Naturkundemuseum in Stuttgart, for the supply of fish teeth as well as the sediment sample from the fish layer. Bettina Reichenbacher, Universität München, is acknowledged for the determination of the fish otoliths and Wolfgang Witt for the supply of some ostracod specimens. Furthermore, we appreciate getting access to the clean lab and the TIMS at the Institut für Geowissenschaften, Universität Tübingen, given to us by Muharrem Satir and Wolfgang Siebel. Elmar Reitter, Universität Tübingen, is acknowledged for some of the Sr isotope measurements. Modern karst water samples from the Steinheim basin as well as air temperature and precipitation data were kindly supplied by Peter Seidel and Eberhard Stabenow, Steinheim. Philippe Thelin, Université de Lausanne, and Gisela Bartholomä, Universität Tübingen, are thanked for XRD analyses of the gastropod shells, and Pascal Tschudin, Université de Laussane, for making the SEM pictures. The National Isotope measurement network of Switzerland (NISOT) is acknowledged for supplying up-to-date oxygen isotope and air temperature data of Switzerland. This study was funded by the Swiss National Science Foundation grant 200021-100530/1 to TWV. We thank A. Longinella and S.T. Grimes for their helpful reviews.

References

Ayliffe, L.K., Lister, A.M., Chivas, A.R., 1992. The preservation of glacial–interglacial climatic signatures in the oxygen isotopes of elephant skeletal phosphate. Palaeogeogr. Palaeoclimatol. Palaeoecol. 99, 179–191.

Bahrig, B., Mensik, H., Mergelsberg, W., 1986. Das Steinheimer Becken (Süddeutschland); Erläuterungen zu einer geologischen Karte 1:10.000. Boch. geol. Geotech. Arb. 21, 1–31.

Bajor, M., 1965. Zur Geochemie der tertiären Süβwasserablagerungen des Steinheimer Beckens, Steinheim am Albuch (Württemberg). Jh. geol. Landesamt Baden-Württ., vol. 7, pp. 355–386.

Barrick, R.E., Fischer, A.G., Showers, W.J., 1999. Oxygen isotopes from turtle bone: applications for terrestrial paleoclimates? Palaios 14, 186–191.

Bausch, W.M., 1965. Strontiumgehalte in süddeutschen Malmkalken. Geol. Rundsch. 55, 86–96.

Bausch, W.M., Hoefs, J., 1972. Die Isotopenzusammensetzung von Dolomiten und Kalken aus dem süddeutschen Malm. Contrib. Mineral. Petrol. 37, 121–130.

Bentley, R.A., Knipper, C., 2005. Geographic patterns in biologically-available strontium, carbon, and oxygen isotope signatures in prehistoric SW Germany. Archaeometry 47, 629–644.

Berggren, W.A., Kent, D.V., Swisher, C.C., Aubry, M.-P., 1995. A revised Cenozoic geochronology and chronostratigraphy. In: Berggren, W.A., Kent, D.V., Aubry, M.-P., Hardenbol, J. (Eds.), Geochronology, Time Scales and Global Stratigraphic Correlation, vol. 54. SEPM Spec. Publ., Tulsa, pp. 129–212.

Blum, J.D., Taliaferro, E.H., Weisse, M.T., Holmes, R.T., 2000. Changes in Sr/Ca, Ba/Ca and $^{87}Sr/^{86}Sr$ ratios between two forest ecosystems in the northeastern USA. Biogeochemistry 49, 87–101.

Böhme, M., 2003. The Miocene climatic optimum: evidence from ectothermic vertebrates of Central Europe. Palaeogeogr. Palaeoclimatol. Palaeoecol. 195, 389–401.

Böhme, M., 2004. Migration history of air-breathing fishes reveals Neogene atmospheric circulation patterns. Geology 32, 393–396.

Böhme, M., Gregor, H.J., Heissig, K., 2001. The Ries and Steinheim meteorite impacts and their effect on environmental conditions in time and space. In: Buffetaut, E., Koerbel, C. (Eds.), Geological and Biological Effects of Impact Events. Springer Verlag, Berlin, Heidelberg, New York, pp. 215–235.

Bryant, J.D., Froelich, P.N., 1995. A model of oxygen isotope fractionation in body water of large mammals. Geochim. Cosmochim. Acta 60, 4523–4537.

Bryant, J.D., Koch, P.L., Froelich, P.N., Showers, W.J., Genna, B.J., 1996. Oxygen isotope partitioning between phosphate and carbonate in mammalian apatite. Geochim. Cosmochim. Acta 60, 5145–5148.

Buchard, B., 1978. Oxygen isotope palaeotemperatures from the Tertiary period in the North Sea area. Nature 275, 121–123.

Buchner, E., Seyfried, H., van den Bogaard, P., 2003. $^{40}Ar/^{39}Ar$ laser probe age determination confirms the Ries impact crater as the source of glass particles in Graupensand sediments (Grimmelfingen Formation, North Alpine Foreland Basin). Int. J. Earth Sci. 92, 1–6.

Cerling, T.E., Harris, J.M., 1999. Carbon isotope fractionation between diet and bioapatite in ungulate mammals and implications for ecological and paleoecological studies. Oecologia 120, 347–363.

Cerling, T.E., Solomon, K.D., Quade, J., Bowman, J.R., 1991. On the isotopic composition of carbon in soil carbon dioxide. Geochim. Cosmochim. Acta 55, 3403–3405.

Cerling, T.E., Harris, J.M., MacFadden, B.J., Leakey, M.G., Quade, J., Eisenmann, V., Ehleringer, J.R., 1997. Global vegetation change through the Miocene/Pliocene boundary. Nature 389, 153–158.

Craig, H., 1953. The geochemistry of the stable carbon isotopes. Geochim. Cosmochim. Acta 3, 53–92.

Craig, H., Gordon, L.I., Horibe, Y., 1963. Isotopic exchange effects in the evaporation of water: 1. Low temperature experimental results. J. Geophys. Res. 68, 5079–5087.

D'Angela, D., Longinelli, A., 1990. Oxygen isotopes in living mammal's bone phosphate: further results. Chem. Geol. 86, 75–82.

Dansgaard, W., 1964. Stable isotopes in precipitaion. Tellus 16, 436–468.

Degens, E.T., Steven, L., 1965. Comparative studies of amino-acids in shell structures of *Gyraulus trochiformis*, Stahl, from the Tertiary of Steinheim, Germany. Nature 205, 876–878.

Deines, P., 1980. The isotopic composition of reduced organic carbon. In: Fritz, P., Fontes, C. (Eds.), Handbook of Environmental Geochemistry, vol. 1. Elsevier, New York, pp. 239–406.

Dettmann, I., Kohn, M., Quade, J., Reyerson, F.J., Ojah, T.P., Hamidullah, S., 2001. Seasonal stable isotope evidence for a strong Asian monsoon throughout the past 10.7 Ma. Geology 29, 31–34.

Dietz, R.S., 1959. Shatter cones in cryptoexplosion structures (meteorite impact?). Geology 67, 496–505.

Eberhard, M., 1989. Klimaänderungen vom Mittel- bis Obermiozän aufgrund makroskopischer Pflanzenreste in Altwaser-Ablagerungen der Adelegg (Allgäu). Geol. Bavarica 94, 459–484.

Engelhardt v., W., Bertsch, W., Stöffler, D., 1967. Anzeichen für den meteoritischen Ursprung des Beckens von Steinheim. Naturwissenschaften 54, 198–199.

Engelhardt v., W., Luft, E., Arndt, J., Schock, H., 1987. Origin of moldavites. Geochim. Cosmochim. Acta 51, 1425–1443.

Epstein, S., Buchsbaum, R., Lowenstamm, H.A., Urey, H.C., 1953. Revised carbonate-water isotopic temperature scale. Bull. Geol. Soc. Am. 64, 1315–1326.

Fahlbusch, V., 1976. Report on the international symposium on mammalian stratigraphy of the European Tertiary. Newsl. Stratigr. 5, 160–167.

Farquhar, G.D., Ehleringer, J.R., Hubrick, K.T., 1989. Carbon isotope fractionation and photosynthesis. Annu. Rev. Plant Physiol. Mol. Biol. 44, 503–537.

Finger, I., 1998. Gastropoden der kleini-Schichten des Steinheimer Beckens (Miozän, Süddeutschland). Stuttg. Beitr. Naturkd., B 259, 1–51.

Flower, B.P., Kennett, J.P., 1994. The Middle Miocene climate transition: East Antarctic ice sheet development, deep ocean circulation and global carbon cycling. Palaeogeogr. Palaeoclimatol. Palaeoecol. 108, 537–555.

Fricke, H.C., O'Neil, J.R., 1996. Inter- and intra-tooth variation in the oxygen isotope composition of mammalian totth enamel phosphate: implications for paleoclimatological and palaeobiological research. Palaeogeogr. Palaeoclimatol. Palaeoecol. 126, 91–99.

Fricke, H.C., Clyde, W.C., O'Neil, J.R., 1998. Intra-tooth variations in $\delta^{18}O$ (PO_4) of mammalian tooth enamel as a record of seasonal variations in continental climate variables. Geochim. Cosmochim. Acta 62, 1839–1850.

Fritz, P., Poplawski, S., 1974. ^{18}O and ^{13}C in the shells of freshwater molluscs and their environments. Earth Planet. Sci. Lett. 91–98.

Gat, J.R., 1995. Stable isotopes of fresh and saline lakes, In: Lerman, A., Imboden, D., Gat, J. (Eds.), Physics and Chemistry of Lakes, 2nd edition. Springer, New York, Heidelberg, pp. 217–263.

Gaudant, J., 1989. Nouvelles observations sur l´ichthyofaune miocène de Steinheim am Albuch (Wurtemberg, Allemagne). Stuttg. Beitr. Naturkd., B 151, 1–33.

Gentner, W., Wagner, G.A., 1969. Altersbestimmungen an Riesgläsern und Moldaviten. Geol. Bavarica 61, 296–303.

Gentner, W., Lippolt, H.J., Schaeffer, O.A., 1963. Das Kalium-Argon-Alter der Gläser des Nördlinger Rieses und der böhmisch-mährischen Tektite. Geochim. Cosmochim. Acta 27, 191–200.

Geyer, O.F., Gwinner, M.P., 1991. Geologie von Baden-Württemberg, 4th edition. Schweizerbart, Stuttgart. 482 pp.

Gonfiantini, R., 1986. Environmental isotopes in lake studies. In: Fritz, P., Fontes, J.Ch. (Eds.), Handbook of Environmental Isotope Geochemistry. Elsevier, Amsterdam, pp. 113–168.

Gorthner, A., 1992. Bau, Funktion und Evolution komplexer Gastropodenschalen in Langzeit-Seen Mit einem Beitrag zur Paläobiologie von *Gyraulus*, *multiformis"* im Steinheimer Becken. Stuttg. Beitr. Naturkd., B 190, 1–173.

Gorthner, A., Meier-Brook, C., 1985. The Steinheim basin as palaeoancient lake. In: Bayer, U., Seilacher, A. (Eds.), Sedimentary and Evolutionary Cycles. Lecture Notes in Earth Sciences, vol. 1. Springer Verlag, Berlin, Heidelberg, pp. 322–334.

Graustein, W.C., 1989. $^{87}Sr/^{86}Sr$ ratios measure the sources and flow of strontium in terrestrial ecosystems. In: Rundel, P.W., Ehleringer, J. R., Nagy, K.A. (Eds.), Stable Isotopes in Ecological Research. Springer-Verlag, New York, pp. 491–512.

Gregor, H.-J., 1983. Die miozäne Blatt-und Frucht-Flora von Steinheim am Albuch (Schwäbische Alb). Doc. Nat. 10, 1–45.

Grimes, S.T., Mattey, D.P., Hooker, J.J., Collinson, M.E., 2003. Palaeogene palaeoclimate reconstruction using oxygen isotopes from land and freshwater organisms: the use of multiple palaeoproxies. Geochim. Cosmochim. Acta 67, 4033–4047.

Grimes, S.T., Hooker, J.J., Collinson, M.E., Mattey, D.P., 2005. Summer temperatures of late Eocene to early Oligocene freshwaters. Geology 33, 189–193.

Groschopf, P., Reiff, W., 1969. Das Steinheimer Becken. Ein Vergleich mit dem Ries. Geol. Bavarica 61, 400–412.

Grossmann, E.L., Ku, T.-L., 1986. Oxygen and carbon isotope fractionation in biogenic aragonite: temperature effects. Chem. Geol. 59, 59–76.

Hart, W., Quade, J., Madsen, D.B., Kaufmann, D.S., Oviat, 2004. The $^{87}Sr/^{86}Sr$ ratios of lacustrine carbonates and lake-level history of the Bonneville paleolake system. Bull. Geol. Soc. Am. 116, 1107–1119.

Heissig, K., 1995. Die Entwicklung der großen *Democricetodon*-Arten und die Gattung *Collimys* (Cricetidae, Mamm.) im späten Mittelmiozän. Mitt. Bayer. Staatsslg. Paläont. hist. Geol. 35, 87–108.

Heissig, K. 2005. Personal observation in the field.

Heizmann, E.P.J., 1973. Die Carnivoren des Steinheimer Beckens.B. Ursidae, Felidae, Viverridae sowie Ergänzungen und Nachträge zu den Mustelidae. Palaeontographica, Suppl. 8 (5), 1–95.

Heizmann, E.P.J., Fahlbusch, V., 1983. Die mittelmiozäne Wirbeltierfauna vom Steinberg (Nördlinger Ries). Eine Übersicht. Mitt. Bayer. Staatssamml. Paläontol. Hist. Geol. 23, 83–92.

Heizmann, E.P.J., Hesse, A., 1995. Die mittelmiozäne Vogel- und Säugetierfaunen des Nördlinger Ries (MN 6) und des Steinheimer Beckens (MN 7) - ein Vergleich. Cour. Forschungsinst. Senckenberg 181, 171–185.

Heizmann, E.P.J., Reiff, W., 2002. Der Steinheimer Meteorkrater. Verlag Dr. Friedrich Pfeil, München. 160 pp.

Hilgendorf, F., 1866. Planorbis multiformis im Steinheimer Süsswasserkalk. Ein Beispiel von Gestaltveränderung im Laufe der Zeit. Buchhandlung W.Weber, Berlin. 36 pp.

Hillson, S., 2005. Teeth, 2nd edition. Cambridge University Press, Cambridge, p. 373.

Hoppe, K.A., Koch, P.L., Carlson, R.W., Webb, S.D., 1999. Tracking mammoths and mastodons: reconstruction of migratory behavior using strontium isotope ratios. Geology 27, 439–442.

Hoppe, K.A., Stover, S.M., Pascoe, J.R., Amundson, S.D., 2004. Patterns of tooth enamel biomineralization in modern domestic horses: implications for isotopic microsampling. Palaeogeogr. Palaeoclimatol. Palaeoecol. 206, 355–365.

Horn, P., Müller-Sohnius, D., Köhler, H., Graup, G., 1985. Rb–Sr systematics of rocks related to the Ries Crater, Germany. Earth Planet. Sci. Lett. 75, 384–392.

Horwarth, T. 2000. Strontium-Isotopensystematik an Sedimentgesteinen der Germanischen Trias und Mineralwässern aus Stuttgart und Umgebung, Unpublished Diploma thesis. Ludwig-Maximilians-Universität München. 77 pp.

Huertas, A.D., Iacumin, P., Stenni, B., Chillon, B.S., Longinelli, A., 1995. Oxygen isotope variations of phosphate in mammalian bone and tooth enamel. Geochim. Cosmochim. Acta. 59, 4299–4305.

Iacumin, P., Bocherens, H., Mariotti, A., Longinelli, A., 1996. Oxygen isotope analyses of co-existing carbonate and phosphate in biogenic apatite: a way to monitor diagenetic alteration of bone phosphate. Earth Planet. Sci. Lett. 142, 1–6.

Jankowski, B., 1981. Die Geschichte der Sedimentation im Nördlinger Ries und Randecker Maar. Boch. Geol. Geotech. Arb., Heft 6, 315.

Janz, H., 1992. Die miozänen Süsswasserostrakoden des Steinheimer Beckens (Schwäbische Alb, Süddeutschland). Stuttg. Beitr. Naturkd., B 183, 1–117.

Janz, H., 1997. Die Ostrakoden der kleini-Schichten des miozänen Kratersees von Steinheim am Albuch (Süddeutschland). Stuttg. Beitr. Naturkd., B 251, 1–101.

Janz, H., 1998. Muschelkrebse - Zeit- und Umweltzeugen im Tertiär. In: Heizmann, E.P.J. (Ed.), Erdgeschichte mitteleuropäischer Regionen, vol. 2. Vom Schwarzwald zum Ries, Verlag Dr. Friedrich Pfeil, München, pp. 191–198.

Janz, H., 1999. Hilgendorf´s planorbid tree — the first introduction of Darwin´s theory of transmutation into palaeontology. Paleontol. Res. 3, 287–293.

Janz, H., 2000. An example of intralacustrine evolution at an early stage: the freshwater ostracods of the Miocene crater lake of Steinheim (Germany). Hydrobiologia 419, 103–117.

Janz, H., Vennemann, T.W., 2005. Isotopic composition (O, C, Sr, and Nd) and trace element ratios (Sr/Ca, Mg/Ca) of Miocene marine and barckish ostracods from North Alpine Foreland deposits (Germany and Austria) as indicators for palaeoclimate. Palaeogeogr. Palaeoclimatol. Palaeoecol. 225, 216–247.

Jernvall, J., Fortelius, M., 2002. Common mammals drive the evolutionary increase of hypsodonty in the Neogene. Nature 417, 538–540.

Jones, L.M., Faure, G., 1978. A study of strontium isotopes in lakes and surficial deposits of the ice-free valleys, southern Victoria Land, Antarctica. Chem. Geol. 22, 107–120.

Koch, P.L., 1998. Isotopic reconstruction of past continental envrionments. Annu. Rev. Earth Sci. 26, 573–613.

Koch, P.L., Tuross, N., Fogel, M.L., 1997. The effects of sample treatment and diagenesis on the isotopic integrity of carbonate in biogenic hydroxylapatite. J. Archaeol. Sci. 24, 417–429.

Kohn, M., 2004. Comment: tooth enamel mineralization in ungulates: implications for recovering a primary isotopic time-series, by B. H. Passey and T. E. Cerling 2002. Geochim. Cosmochim. Acta 68, 403–405.

Kohn, M.J., Cerling, T.E., 2002. Stable isotope compositions of biological apatite. Phosphates: geochemical, geobiological, and materials importance. In: Kohn, M.J., Rakovan, J., Hughes, J. M. (Eds.), Reviews in Mineralogy and Geochemistry, vol. 48, pp. 455–488.

Kroopnick, P., Weiss, R.F., Craig, H., 1972. Total CO_2, ^{13}C, and dissolved oxygen-^{18}O at Geosecs II in the North Atlantic. Earth Planet. Sci. Lett. 16, 103–110.

Lear, C.H., Elderfield, H., Wilson, P.A., 2000. Cenozoic deep-sea temperatures and global ice volumes from Mg/Ca in benthic foraminiferal calcite. Science 287, 269–272.

Lindars, E.S., Grimes, S.T., Mattey, D.P., Collinson, M.E., Hooker, J. J., Jones, T.P., 2001. Phosphate $\delta^{18}O$ determination of modern rodent teeth by direct laser fluorination: an appraisal of methodology and potential application to palaeoclimate reconstruction. Geochim. Cosmochim. Acta 65, 2535–2548.

Livingstone, D.M., Lotter, A., 1998. The relationship between air and water temperatures in lakes of the Swiss Plateau: a case study with palaeolimnological implications. J. Paleolimnol. 19, 181–198.

Longinelli, A., 1984. Oxygen isotopes in mammal bone phosphate: a new tool for palaeoclimatological and palaeoenvironmental research? Geochim. Cosmochim. Acta 48, 385–390.

Longinelli, A., 1995. Stable Isotope ratios in phosphate in mammal bone and tooth as climatic indicators. In: Frenzel, B., Stauffer, B., Weiβ, M.M. (Eds.), Problems of Stable Isotopes in Tree Rings, Lake Sediments and Peat Bogs as Climatic Evidence for the Holocene. Fischer Verlag, Stuttgart, Jena, New York, pp. 58–70.

Longinelli, A., Nuti, S., 1973. Revised phosphate-water isotopic temperature scale: Earth Planet. Sci. Lett. 19, 373–376.

Longinelli, A., Edmond, J.M., 1983. Isotope geochemistry of the Amazon basin: a reconnaissance. J. Geophys. Res. 88 (C6), 3703–3717.

Lücke, A., Helle, G., Schleser, G.H., Figueiral, I., Mosbrugger, V., Jones, T.P., Rowe, N.P., 1999. Environmental history of the German lower Rhine embayment during the Middle Miocene as reflected by carbon isotope in brown coal. Paleogeogr. Palaeoclimatol. Palaeoecol. 154, 339–352.

Luz, B., Kolodny, Y., 1985. Oxygen isotope variations in phosphate of biogenic apatites: IV. Mammal teeth and bones. Earth Planet. Sci. Lett. 75, 29–36.

Luz, B., Kolodny, Y., Horowitz, M., 1984. Fractionation of oxygen isotopes between mammalian bone-phosphate and environmental drinking water. Geochim. Cosmochim. Acta 48, 1689–1693.

MacFadden, B.J., Solounias, N., Cerling, T.E., 1999. Ancient diets, ecology, and extinction of 5-million-year-old horses from Florida. Science 283, 824–827.

Markwick, P.J., 1998. Fossil crocodilians as Indicators of Late Cretaceous and Cenozoic climates: implications for using palaeontological data in reconstructing palaeoclimate. Palaeogeogr. Palaeoclimatol. Palaeoecol. 137, 205–271.

McArthur, J.M., Howarth, R.J., Bailey, T.R., 2001. Strontium isotope stratigraphy: LOWESS Version 3. Best-fit line to the marine Sr-isotope curve for 0 to 509 Ma and accompanying look-up table for deriving numerical age. J. Geol. 109, 155–169.

Mensink, H., 1984. Die Entwicklung der Gastropoden im miozänen See des Steinheimer Beckens (Süddeutschland). Palaeontographica, A 183, 1–63.

Miller, K.G., Wright, J.D., Fairbanks, R.G., 1991. Unlocking the Ice House: Oligocene–Miocene oxygen isotopes, eustasy, and margin erosion. J. Geophys. Res. 96, 6829–6848.

Mlynarski, M., 1980. Die tertiären Wirbleltiere des Steinheimer Beckens, Teil II, B. Die Schildkröten des Steinheimer Beckens B. Chelydridae mit einem Nachtrag zu den Testudinoidea. Palaeontographica Supl. VIII, Teil II, 1–35.

Mook, W.G., Bommerson, J.C., Staverman, W.H., 1974. Carbon isotope fractionation between dissolved bicarbonate and gaseous carbon dioxide. Earth Planet. Sci. Lett. 22, 169–176.

Müller, W., Fricke, H., Halliday, A.N., McCulloch, M.T., Wartho, J.-A., 2003. Origin and migration of the Alpine Iceman. Science 302, 862–866.

Neat, P.L., Faure, G., Pegram, W.J., 1979. The isotopic composition of strontium in non-marine carbonate rocks: the Flagstaff Formation of Utah. Sedimentology 26, 271–282.

Pache, M., Reitner, J., Arp, G., 2001. Geochemical evidence for the formation of a large Miocene "travertine" mound at a sublacustrine spring in a soda lake (Wallerstein castle rock, Nördlinger Ries, Germany). Facies 45, 211–230.

Patterson, W.P., 1999. Oldest isotopically characterised fish otoliths provide insights to Jurassic continental climate in Europe. Geology 27, 199–202.

Patterson, W.P., Smith, G.R., Lohmann, K.C., 1993. Continental paleothermometry and seasonality using the isotopic composition of aragonite otoliths of fresh water fishes. In: Swart, P.K., Lohmann, K.C., McKenzie, J., Swart, S. (Eds.), Climate Change in Continental Isotopic Records. American Geophysical Union Monograph, vol. 78, pp. 191–202.

Price, T.D., Burton, J.H., Bentley, R.A., 2002. The characterization of biologically available strontium isotope ratios for the study of prehistoric migration. Archaeometry 44, 117–135.

Quade, J., Cerling, T.E., Barry, J.C., Morgan, M.E., Pilbeam, D.R., Chivas, A.R., Lee Thorp, J.A., van der Merwe, N.J., 1992. A 16-Ma record of paleodiet using carbon and oxygen isotopes in fossil teeth from Pakistan. Chem. Geol. 94, 183–192.

Reiff, W., 1976. Einschlagkrater kosmischer Körper auf der Erde. In: Meteorite und Meteorkrater. Stuttg. Beitr. Naturkd., C 6, 24–47.

Reiff, W., 1988. Zur Gleichaltrigkeit der Einschlagkrater (Meteorkrater) des Steinheimer Becken und Nördlinger Ries. Jber. Mitt. Oberrhein. Geol. Ver. NF 70, 383–397.

Retallack, G.J., 2004. Late Miocene climate and life on land in Oregon within a context of Neogene global change. Palaeogeogr. Palaeoclimatol. Palaeoecol. 214, 97–123.

Rothe, P., Hoefs, J., 1977. Isotopen-geochemische Untersuchungen an Karbonaten der Ries-See-Sedimente der Forschungsbohrung Nördlingen, 1973. Geol. Bavarica 75, 59–66.

Rozanski, K., Araguás-Araguás, L., Gonfiantini, R., 1993. Isotopic patterns in modern global precipitation. In: Swart, P.K, Lohmann, K.C, McKenzie, J., Savin, S. (Eds.), Climate Change in continental isotopic records. Geophysical Monograph, vol. 78. American Geophysical Union, pp. 1–36.

Schleich, H.H., 1985. Zur Verbreitung tertiärer und quartärer Reptilien und Amphibien: I. Süddeutschland. Münch. Geowiss. Abh. A 4, 67–149.

Schnetzler, C.C., Philpotts, J.A., Pinson, W.H., 1969. Rubidium–strontium correlation study of moldavites and Ries Crater material. Geochim. Cosmochim. Acta 33, 1015–1021.

Schudack, M., Janz, H., 1997. Die Charophyten der miozänen kleini-Schichten, Hinweise auf Alter und Frühentwicklung des Kratersees von Steinheim am Albuch (Süddeutschland). Sonderveröff. Geol. Inst. Univ. Köln 114, 427–449.

Schumacher, G.-H., Schmidt, H., 1983. Anatomie und Biochemie der Zähne, 3. überarbeitete Aufl., Gustav Fischer Verlag. 569 pp.

Schürch, M., Kozel, R., Schotterer, U., Tripet, J.-P., 2003. Observation of isotopes in the water cycle the Swiss National Network (NISOT). Environ. Geol. 45, 1–11.

Schweigert, G., 1993. Die mittelmiozäne Flora (MN 7) von Steinheim am Albuch (Schwäbische Alb, Baden Württemberg). Jh. Ges. Naturkde. Württemberg 148, 61–96.

Seidel, P., 2005. Meteorological data from the Steinheim basin measured from 1976–2003.

Shanahan, T.M., Pigati, J.S., Dettman, D.L., Quade, J., 2005. Isotopic variability in the aragonite shells of freshwater gastropods living in springs with nearly constant temperature and isotopic composition. Geochim. Cosmochim. Acta 69, 3949–3966.

Sharp, Z.D., Cerling, T.E., 1998. Fossil isotope records of seasonal climate and ecology: straight from the horse's mouth. Geology 26, 219–222.

Shoemaker, E.M., Chao, E.C.T., 1961. New evidence for the impact origin of the Ries basin, Bavaria, Germany. J. Geophys. Res. 66, 3371–3378.

Sillen, A., Hall, G., Richardson, S., Armstrong, R., 1998. $^{87}Sr/^{86}Sr$ ratios in modern and fossil food-webs of the Sterkfontein Valley: implications for early hominid habitat preference. Geochim. Cosmochim. Acta 62, 2463–2473.

Spötl, C., Vennemann, T.W., 2003. Continuous-flow IRMS analysis of carbonate minerals. Rapid Communications in Mass Spectrometry 17, 1004–1006.

Staudacher, T., Jessberger, E.K., Dominik, R.E., Kirsten, E., Schaeffer, O.A., 1982. $^{40}Ar/^{39}Ar$ ages of rocks and glasses form the Nördlinger Ries Crater and the temperature history of impact breccias. J. Geophys. Res. 51, 1–11.

Steininger, F.F., 1999. Chronostratigraphy, geochronology and biochronology of the Miocene "European Land Mammal Mega-Zones" (ELMMZ) and the Miocene "Mammal-Zones (MN-Zones)". In: Rössner, G.E., Heissig, K. (Eds.), The Miocene Land Mammals of Europe. Verlag Dr. Friedrich Pfeil, München, pp. 9–24.

Straight, W.H., Karr, J.D., Cox, J.E., Barrick, R.E., 2004. Stable oxygen isotopes from theropod dinosaur tooth enamel: interlaboratory comparison of results and analytical interference by reference standards. Rapid Commun. Mass Spectrom. 18, 2897–2903.

Swart, P.K., Lohmann, K.C., McKenzie, J., Swart, S., 1993. Climate change in continental isotopic records. Monograph, 78. American Geophysical Union, p. 374.

Talbot, M.R., 1990. A review of the palaeohydrological interpretation of carbon and oxygen isotopic ratios in primary lacustrine carbonates. Chem. Geol. 80, 261–278.

Tütken, T., unpublished data. $\delta^{18}O$–$\delta^{18}O_{H_2O}$ calibration for extantrhinoceros measured by the author.

Tütken, T., Vennemann, T.W., 2005. A 20 Ma record of paleoclimate for Central Europe and mammalian paleodiet on the basis of stable isotope compositions of Oligocene/Miocene mammal teeth from the Northern Alpine Foreland Basin. Geol. Soc. Am. Abstr. Programs 37 (7), 459.

Utescher, T., Moosbruger, V., Ashraf, A.R., 2000. Terrestrial climate evolution in Northwest Germany over the last 25 million years. Palaios 15, 430–449.

Vennemann, T.W., Hegner, E., 1998. Oxygen, strontium and neodymium isotope composition of shark teeth as a proxy for the paleooceanography and paleoclimatology of the northern alpine Paratethys. Palaeogeogr. Palaeoclimatol. Palaeoecol. 142, 107–121.

Vennemann, T.W., Morlok, A., von Engelhardt, W.E., Kyser, T.K., 2001. Stable isotope composition of impact glasses from the Nördlinger Ries impact crater, Germany. Geochim. Cosmochim. Acta 65, 1325–1336.

Vennemann, T.W., Fricke, H.C., Blake, R.E., O´Neil, J.R., Colman, A., 2002. Oxygen isotope analysis of phosphates: a comparison of techniques for analysis of Ag_3PO_4. Chem. Geol. 185, 321–336.

Wachniew, P., Różański, K., 1997. Carbon budget of a mid-latitude, groundwater-controlled lake: Isotopic evidence for the importance of dissolved inorganic carbon recycling. Geochim. Cosmochim. Acta 61, 2453–2465.

Weiler, W., 1934. Die tertiären Wirbeltiere des Steinheimer Beckens, Teil I, Die Fische des Steinheimer Beckens. Palaeontographica Supl. VIII (I), 1–20.

Wolanski, E., Gereta, E., Borner, M., Mduma, S., 1999. Water, migration and the Serengeti ecosystem. Am. Sci. 87, 526–533.

Wolff, M., Füchtbauer, H., 1976. Die karbonatische Randfazies der tertiären Süsswasserseen des Nördlinger Ries und des Steinheimer Beckens. Geol. Jahrb., Reihe D 14, 3–53.

Yang, C., Tellmer, K., Veizer, J., 1996. Chemical dynamics of the St. Lawrence riverine system: δD_{H2O}, $\delta^{18}O_{H2O}$, $\delta^{13}C_{DIC}$, $\delta^{34}S_{SO4}$, and dissolved $^{87}Sr/^{86}Sr$. Geochim. Cosmochim. Acta 46, 2199–2216.

Zachos, J., Pagani, M., Sloan, L., Thomas, E., Billups, K., 2001. Trends, rhythms, and aberrations in global climate 65 Ma to present. Science 292, 686–693.

Zazzo, A., Lécuyer, C., Mariotti, A., 2004. Experimentally-controlled carbon and oxygen isotope exchange between bioapatites and water under inorganic and microbially-mediated conditions. Geochim. Cosmochim. Acta 68, 1–12.

Zeebe, R.E., Wolf-Gladrow, D.A., Jansen, H., 1999. On the time required to establish chemical and isotopic equilibrium in the carbon dioxide system in seawater. Mar. Chem. 65, 135–153.